Modeling and Analysis on Pervaporation Separation of Composite Zeolite Membranes

by

Stewart Mann

A Thesis Presented in Partial Fulfillment
of the Requirements for the Degree
Master of Science

Approved July 2014 by the
Graduate Supervisory Committee:

Jerry Lin, Chair
Mary Lind
David Nielsen

ARIZONA STATE UNIVERSITY

August 2014

ABSTRACT

Pervaporation is a membrane separation technology that has had industrial application and which is the subject of ongoing research. Two major factors are important in judging the quality of a membrane: selectivity and permeation flux. Although many types of materials can be used for the separation layer, zeolites will be the material considered in this thesis. A simple mathematical model has been developed to demonstrate the inter-relationships between relative permeation flux, reduced selectivity, and the relative resistance to mass transfer of the support to the zeolite layer. The model was applied to several membranes from our laboratory and to two examples from the literature. The model offers a useful way of conceptualizing membrane performance and facilitates the comparison of different membrane performances. The model predicts the effect of different supports on zeolite supported membrane performance.

ACKNOWLEDGMENTS

I would first like to thank my thesis advisor, Professor Jerry Lin, for all his help and guidance. I am very grateful for the opportunity to be a member of Professor Lin's research group.

I would like to thank Professor Lind and Professor Nielsen for serving on my committee.

I would like to thank the faculty at ASU. The quality of teaching has been excellent in all respects.

I would like to thank Xiaoli Ma for all his help and support.

A special thanks to my wife Candice, and my two sons Matthew and Gabriel.

I would also like to thank my current and former group members: Xueliang Dong, Wangliang Mi, Alexandra Kasik, Nick Linneen, Amr Ibrahim, Joshua James, Yang Liu, Hong Mang, Xiaojuan Hu, BoLu, Defei Liu, Huifang Zhang, Hu Xiaojuan, Tyler Norton

TABLE OF CONTENTS

Page

CHAPTER Page

CHAPTER Page

LIST OF TABLES

LIST OF FIGURES

CHAPTER 1

INTRODUCTION

1.1 MEMBRANE SEPARATION PROCESSES

1.1.1 General Background

Membrane separations have become important in chemical engineering as this type of separation can replace or supplement other separation modalities. Continuous membrane processes for liquid separations provide an alternative to complex and energy intensive separation processes such as selective adsorption, azeotropic distillation or cryogenic distillation [1]. Selecting a separation modality, on an industrial scale, is largely based on cost, including the amount of energy required, and feasibility. Various criteria can be used to classify membranes used for separation. A list based on the type of process includes: [2]

1. Microfilitration
2. Ultrafiltration
3. Electrodialysis
4. Reverse osmosis
5. Hemodialysis
6. Gas separation
7. Pervaporation

The underlying concept in membrane separations is that the membrane forms a semipermeable barrier which favors the transport of one species in a mixture over others through the membrane. The driving force for transport of a species is its chemical potential gradient across the membrane. The driving force can also be expressed as the

pressure difference, high to low, from the feed side to the permeate side, of the permeating species. The flow of the mixture, or its components, through the membrane is called flux. The units of flux are $\frac{Kg}{m^2 Hr}$ or $\frac{mol}{m^2 s}$ where the area in the denominator is the surface area of the membrane usually normal to the direction of flow. Selectivity is one way of describing the ability of a membrane to separate species in the feed mixture. Selectivity is defined as the ratio of the permeance of the main permeating component to the permeance of the other mixture component, and is dimensionless. Separation factor is also commonly used in the pervaporation literature to describe the ability of a membrane to separate the species in the feed. Separation factor is defined as $\frac{wgt_{i,permeate}}{wgt_{j,permeate}} \Big/ \frac{wgt_{i,feed}}{wgt_{j,feed}}$. Moles, concentrations, or mole fractions can be used in place of weights with the same result. The separation factor is affected by the properties of the membrane, the vapor-liquid equilibrium diagram of the feed solution (including feed composition), and the process operating conditions. Selectivity reflects the intrinsic properties of the membrane. Using selectivity as the measure of the ability of the membrane to separate the species also allows comparison to gas permeation studies. For these reasons, it is the preferred way of reporting separation ability [2]. Industrial applications of membrane separations often require both high flux and high selectivity. High selectivity means high product purity and high energy efficiency. The flux and selectivity are determined in most cases by a solution diffusion mechanism. The materials from the feed are adsorbed, or dissolve, onto the membrane surface, and then diffuse through the membrane pores to the permeate side. Another mechanism of

separation is molecular sieving where the mixture components are separated based on the pore diameter of the membrane allowing the transport of one the feed species, but excluding the other based on size. Membranes for separation can be broadly classified as polymeric or inorganic based on composition. They are also classified based on pore size as microporous (< 2nm pore diameter), mesoporous (2-100 nm pore diameter), and macroporous (>100 nm pore diameter).

1.1.2 **Pervaporation**

The feed in pervaporation is a liquid, the permeate is a vapor maintained at low partial pressure by means of a sweep gas or vacuum. Pervaporation is usually described as a three step process: solution-diffusion-evaporation (on the permeate side) [3]. The vapor permeate is then condensed to a liquid.

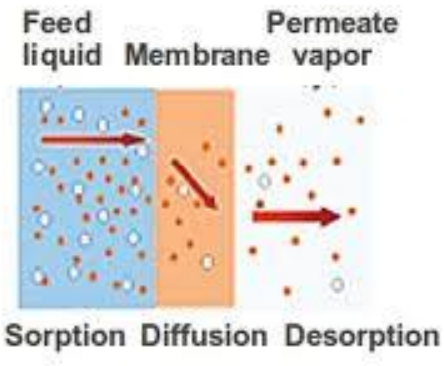

Figure 1.1

Flow through a membrane in pervaporation

Pervaporation for liquid separations provides three advantages over other liquid separation modalities [1]:

1. Reduced energy demand because only a fraction of the feed needs to be vaporized.
2. Continuous operation
3. Higher driving force because of the downstream vacuum (or sweep gas).

According to Baker, pervaporation originated in the 19th century and the term was coined by Kober in 1917. The process was first studied in systematic fashion in the 1950s by American Oil. By the 1980s advances in membrane technology made it possible to prepare economically viable pervaporation systems. [2]

The most important current industrial application of pervaporation is the removal of water from organic solvents, most importantly ethanol. Pervaporative dehydration of ethanol typically produces a product containing less than 1% water from a feed containing 10% water. It is not possible to achieve this by simple distillation since ethanol and water form an azeotrope at about 95% ethanol. One of the industrial leaders in applying pervaporation technology is Sulzer Chemtech (GFT membranes). They have installed about 200 small plants mostly to remove water from ethanol and isopropyl alcohol streams for the pharmaceutical and fine chemical industries. [2] Amorphous (noncrystalline) microporous silica membranes are used by Sulzer to obtain ethanol containing < 1% water. As a blend for gasoline, the water content for ethanol must be reduced to 2000 ppm, for ethyl tertiary butyl ether production the water content of ethanol must be <500 ppm. The hydrophilic NaA (**LTA** structure) zeolite (crystalline microporous) membrane is extremely selective in the pervaporation separation of water from ethanol and can achieve purity in the order of 500 ppm. One example of the performance of this membrane from the literature [4] showed a flux of 5.60 $\frac{Kg}{m^2 Hr}$ and a

separation factor >5000. The use of NaA zeolite membrane, by Mitsui Engng. & Shipbuilding Corp. represents the only large scale industrial application of zeolite membranes in pervaporation. [5,6,7]

The number of industrial applications of pervaporation is limited. However research efforts suggest several areas of potential usage on an industrial scale:

1. Water and wastewater treatment
2. Food and biotechnology sector
3. The recovery of aroma compounds
4. The removal of toxic organics from industrial effluents
5. The petrochemical industry (desulfurization of FCC gasoline)
6. The removal of methanol from MTBE
7. The removal of ethanol from wine and beer
8. The removal of ethanol from fermentation broth (biofuel)

The removal of ethanol from fermentation broth is an organic-water separation. Polymer membranes have been investigated for this separation; however zeolite (silicalite-1) membranes produce higher fluxes and separation factors [8]. A large amount of ongoing research has investigated the use of organophilic **MFI** zeolite membranes for this pervaporative separation. This thesis will focus on the use of **MFI** zeolite silicalite-1 for ethanol/water separation. Subsequent sections will describe zeolites, silicalite-1, zeolite membranes, and **MFI** zeolite separations.

1.2 **ZEOLITE MEMBRANES**

1.2.1 **Zeolites**

Zeolites are aluminosilicate framework crystalline structures which can be represented by the formula: $M_{2/n}O.Al_2O_3.xSiO_2.yH_2O$ where n is the cation valence. The basic structural unit in zeolites is a TO 4 regular tetrahedron formed of a tetrahedrally ccoordinated atom (the "T" atom, often silicon) located at the center of four oxygen atoms which form the vertices of the tetrahedron. The tetrahedra are corner linked by oxygen bridges containing 8, 10, or 12 oxygen atoms to form periodic frameworks, usually displaying channels (pores) in one or more dimensions. The number of oxygen atoms in the bridge determines the pore size of the zeolite. Each framework type is uniquely defined by the way the comprising tetrahedra are linked. There are currently over 200 zeolite topologies recognized to exist as real materials by the Structure Commission of the International Zeolite Association (IZA). Each of the known framework types is assigned a boldface three letter code by the IZA that defines the structure but not necessarily the type of material. In some cases, the code is derived from the name of the first material found to exhibit the framework topology. Many types of materials are represented within the 200+ framework types. About 20% of the framework types have been synthesized as pure silicates. Silicon atoms are often replaced by aluminum, germanium, phosphorous, or boron atoms, among others. When a trivalent atom replaces silicon, other extra-framework cations are required to preserve electroneutrality. One significant consequence of this type of substitution is that the hydrophilicity of the zeolite changes, zeolites with high silicon content being relatively

hydrophobic (organophilic) [9]. Details of each zeolite structure can be found on the official IZA website.

For the purpose of this thesis, it is sufficient to state that the **MFI** structure has 10 oxygen atoms forming its periodic framework. The pore structure of **MFI** zeolites consists of two channels: straight channels with circular openings of 0.54 nm x 0.56 nm along the *b* axis and sinusoidal channels with elliptical openings of 0.51 nm x 0.55 nm along the α-axis [10]. ZSM-5 (framework type **MFI**) is an aluminosilicate belonging to the pentasil family of zeolites. Its chemical formula is $Na_nAl_nSi_{96-n}O_{192}\cdot 16H_2O$ ($0<n<27$). Silicalite, the aluminum free member of the ZSM-5 family, was first synthesized by Flanigen et. al. in 1978 [11]. A year later the aluminum free member of the ZSM-11 family (**MEL** framework) was synthesized by Bibby et. al. and the ZSM-5 aluminum free analogue was named silicalite-1 while the ZSM-11 aluminum free analogue was named silicalite-2 [12].

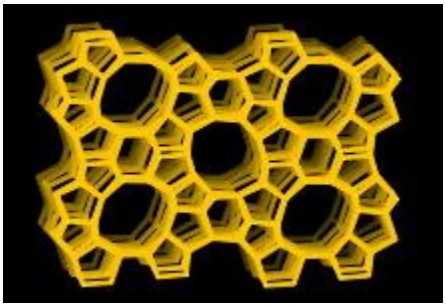

Figure 1.2

***MFI** structure (IZA website)*

Cronstedt coined the term zeolite in 1756 after he observed that on heating a natural zeolite mineral (aluminosilicate), the material appeared to bubble as water was lost as steam from the zeolite (pores). Cronstedt had discovered a class of materials that were not just porous, but that had pores and cavities of molecular dimensions. In 1857 Damour demonstrated that the water loss was reversible. In 1862 Deville synthesized the first zeolite (Deville is also known for his preparation of aluminum and its display at the 1855 Paris Exposition). In 1905 zeolites were used commercially as water softeners. In 1948 Barrer synthesized ZK-5, a zeolite with no known natural counterpart, and for the first time industrial use of zeolites did not depend on scarce and impure natural deposits. The term "zeolite" was loosely used in the first part of the 20th century to include carbonaceous materials and amorphous aluminosilicates. In 1967 Barrer became one of the cofounders of the International Zeolite Association.

Figure 1.3

Richard Maling Barrer

Through the 1950s, the main commercial use of zeolites was in adsorption and separation applications. In the 1960s zeolites became widely used in laundry detergents because of their ion exchange properties. In 1960, Weisz and Frilette at Socony Mobil found unexpected catalytic activity in zeolites. After this, all the large petrochemical companies took a greater interest in zeolites and catalytic applications were developed by them. In 1967 the first high silica zeolite, zeolite beta was synthesized at Mobil by Wadlinger, Kerr, and Rosinski. This zeolite had significant hydrophobicity and catalytic activity, leading to research efforts to develop high silica zeolites. In 1980 Flanigan described the evolution in synthetic zeolite materials from the initial "low silica" zeolites such as A and X through "intermediate silica" zeolites such as Y,L, omega, and synthetic mordenite, to "high silica" organophilic **MFI** zeolites such as ZSM-5 ($Si/Al = 60$) and silicalite-1 ($Si/Al > 300$), and described the resultant gradation in stability, and, properties as adsorbents and catalysts. [13]

In 2001, the world market for synthetic zeolites at about 1.6 million tons, was about half of natural zeolite production. Detergent use accounted for 82% of this production, with catalysts at 8% and desiccants at 5% [13].

1.2.2 **Zeolite Membranes**

It follows that a small percentage of total zeolite production goes towards the production of zeolite membranes for separation. However, it should not be surprising that these remarkable materials are useful in membrane separation technology based on the properties of these materials that have already been described. Additionally, the catalytic properties of zeolites may be combined with their separation properties in the form of membrane reactors [7]. Zeolite membranes are also being developed for

nanoscale applications such as catalytic microreactors, gas sensors, optical sensors, and resonant sensors [14].

Zeolite membranes have several advantages over polymer membranes [15]:

1. Zeolite membranes do not swell, whereas polymeric membranes do.
2. Zeolites have uniform molecular sized pores that cause significant differences in transport rates for some molecules, and allow molecular sieving in some cases.
3. Most zeolite structures are more chemically stable than polymeric membranes, allowing separations of strong solvents or low pH mixtures.
4. Zeolites are stable at high temperatures.

In contrast, zeolite membranes in general cost significantly more to produce than polymer membranes, and zeolite membranes are more brittle than polymers

The first attempts to use zeolites membranes for separation were in the 1970s. These membranes were polymer-zeolite composites with poor chemical and thermal stability. Suzuki reported the first supported zeolite membrane for separation in the 1980s. As of today, only a handful of the known frameworks have been able to be synthesized into separation membranes.

Zeolite membranes are almost always prepared by liquid phase hydrothermal synthesis. In this type of synthesis, a zeolite layer is grown on a porous support from a gel by crystallization at 373-473 K. Important factors in synthesis include:

1. Support chemical composition, structure, and roughness
2. Support position when placed in the gel
3. Gel composition, pH, and temperature

The gel usually contains silicon which can be sodium silicate hydroxide, or a metallo-organic compound such as tetraethyl-orthosilicate (TEOS), and, a source for tetrahedral framework atoms other than silicon (e.g. Sodium aluminate hydroxide). A structural directing agent (SDA) or template such as tetrapropyl ammonium hydroxide is required to make **MFI** zeolites such as ZSM-5 and silicalite-1. The objective is to create a zeolite layer with minimum intercrystalline space (nonzeolite pores) and minimum thickness which is strongly bound to the support. One type of hydrothermal synthesis is in-situ synthesis. In this type, the zeolite layer is grown directly on the support. Another type of synthesis is referred to as secondary growth. In this type a seed layer of zeolite crystals is first deposited on the support by hydrothermal treatment. The seed layer/support is then dried and calcined, then hydrothermally treated a second time to allow zeolite crystal nucleation on the seeds forming a defined layer. After the zeolite layer is formed on the support it is calcined. The template is removed by calcining, opening the zeolite pores. For industrial applications, zeolite membranes must provide high flux and selectivity. Highly selective membranes are often thick so as to minimize intercrystalline defects, while flux is inversely related to membrane thickness [14].

1.2.3 **Separations by Zeolite Membranes**

Ongoing research has demonstrated the ability of the **MFI** zeolite membranes silicalite-1 and ZSM-5, to achieve the following gas separations [10]:

1. n-butane and isobutene
2. Hydrogen and butane
3. Carbon dioxide and nitrogen
4. p-xylene from its isomers

5. Hydrogen and carbon dioxide

These separations are accomplished by the molecular sieving effect. For example, p-xylene can enter the zeolite pores readily, while the other xylene isomers cannot.

Silicalite-1 or ZSM-5 has been able to pervaporatively separate the following organics from water [10]:

1. Methanol
2. Ethanol
3. 1-propyl alcohol
4. Isopropyl alcohol
5. Acetone
6. Acetic acid
7. *P*-Xylene from its isomers

One of the difficulties of *p*-xylene pervaporation separation by **MFI** zeolite membranes is that the **MFI** framework is distorted by high *p*-xylene loading [1]. Framework distortion is not seen in pervaporation separation of ethanol/water.

One of the potential industrial applications of the **MFI** zeolite membranes, separating ethanol from water, is the production of ethanol from fermentation broth [7]. Continuous removal of ethanol from the fermentation broth is desirable because the fermentation process stops at an ethanol concentration of about 15 wgt.% Typical performance with real fermentation broths show fluxes in the order of 1 $\frac{Kg}{m^2 Hr}$ and separation factor of 57. Improvement can be obtained by optimizing the support structure, reducing membrane thickness, and increasing the Si/Al ratio of the **MFI** zeolite membrane. The energy required to deliver a unit of ethanol as condensed permeate is the

sum of the energy required to evaporate and condense both the ethanol and the water. Therefore higher selectivity (or separation factor) is desired to achieve high energy efficiency [8]. Silicalite-1 has the highest Si/Al ratio and has been the subject of research in pervaporative separation of ethanol from water. The results of several investigations are presented in the table below.

Table 1.1

Reported ethanol/water pervaporation performances of silicalite-1 membrane

T (˚C)	Feed EtOH wgt.%	Flux $Kgm^{-2}Hr^{-1}$	Separation Factor	Year	Ref.
30	4	0.31-4.68	1.6-23.4	2002	[16]
30	4.65	0.6	64	1998	[17]
60	5	0.78	57	1994	[18]
60	5	1.8	89	2001	[19]
60	3	2.9	66	2011	[20]
60	5	7.4	47	2012	[21]
60	10	9	5	2013	[22]

The improved fluxes in the Shan and Shu studies were achieved by using hollow fiber supports and the flux reported by Korelsky was achieved using an ultrathin 0.5 μm siliaclite-1 layer. Korelsky cited significant support resistance as a factor which reduced the flux and selectivity. A mathematical model of support resistance developed by de Bruijn et. al. [23] was used to make this determination.

1.3. TRANSPORT MODEL FOR ZEOLITE MEMBRANES

1.3.1 Support Resistance

The meaning of support resistance has to be clarified. If a feed solution is run through a support alone, fluxes may be 10 times higher than the fluxes through a composite zeolite-support membrane. Clearly in this case, the zeolite layer is limiting in terms of flux. From this perspective it would appear that support resistance is negligible or unimportant. However, it is the resistance of the support when the zeolite layer is applied that is important. For this purpose, the interfacial pressure, the pressure at the zeolite-support interface, is the critical parameter.

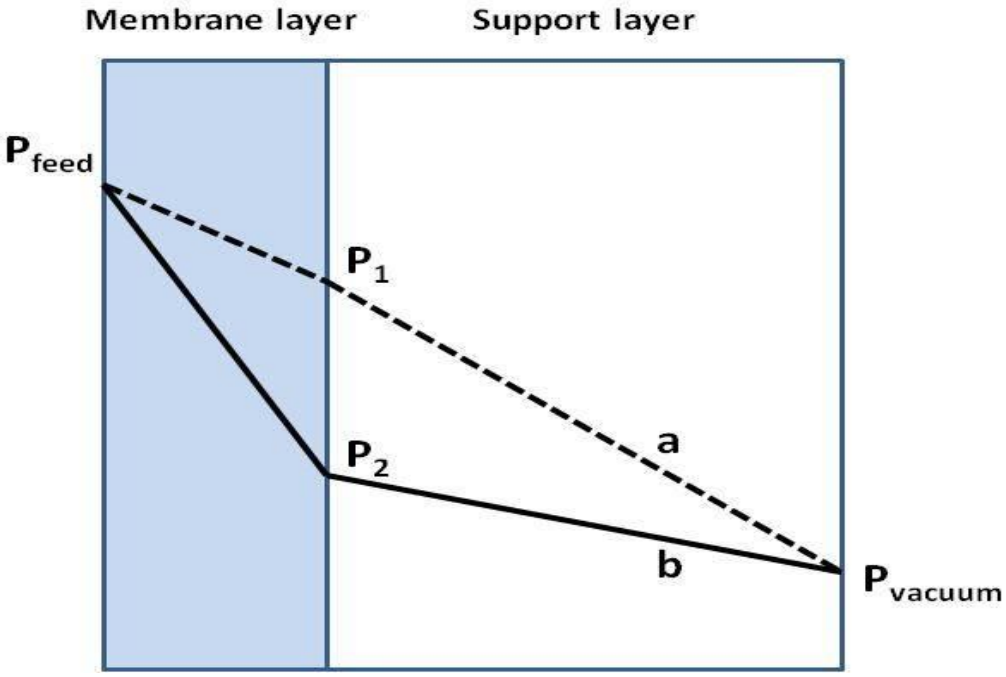

Figure 1.4

Pressure drop across a composite membrane

In figure 1.4, $P_1 and\ P_2$ represent high and low interfacial pressures. Curve (a) represents high support resistance, curve (b) low support resistance

It is possible to calculate the interfacial pressure for any zeolite-support membrane given the feed composition, operating conditions (temperature and permeate pressure), and the support permeance values (α and β). It would then be possible to put the composite zeolite-support membranes into two groups: those with high interfacial pressure and those with low interfacial pressure. If, for example, the interfacial pressures were calculated for the studies of silicalite-1 ethanol/water pervaporative separation listed above, high interfacial pressures would be found [23]. This information may be sufficient. However, if it is desirable to obtain a more complete understanding of the individual performances of the membranes or to compare the performances of these membranes then two quantities would be important. One quantity would be how much flux relative to the theoretical flux of the stand alone zeolite layer (ideal flux) is lost because of support resistance. The second quantity would be how much selectivity is lost because of support resistance relative to the selectivity of the zeolite layer.

1.3.2 **Mathematical Modeling of Transport in the Zeolite Layer**

Mathematical modeling will be useful to address these concerns. To gain an understanding as to how, an overview of current mathematical modeling of the zeolite-support composite membrane will be presented. Mathematical models have been developed to understand and predict the flux and selectivity of the zeolite-support composite membrane. These models consider flux and selectivity through the zeolite layer and through the support separately.

A number of simulation techniques have been used and sometimes combined to describe mixture transport through zeolite membranes. These include Monte-Carlo, molecular dynamics, transition-state theory, Fick and Onsager formulations, and the Maxwell-Stefan model. It is generally accepted that the generalized Maxwell-Stefan formulation offers the most convenient and nearest quantitative prediction of multicomponent diffusion through zeolite membranes. [24]

The generalized Maxwell-Stefan theory conventionally assumes that the movement of a species in a multicomponent mixture is caused by a driving force, the chemical potential gradient, which is balanced by the friction of this species with other species and its surroundings (the zeolite layer) [25]. In the M-S formulation, the chemical potential gradients are written as linear functions of the fluxes:

$$\rho \frac{\theta_i}{RT} \frac{\delta \mu_i}{\delta z} = \sum_{j=1, j \neq i}^{n} \frac{q_j N_i - q_i N_j}{q_{i,sat} q_{j,sat} Đ_{i,j}} + \frac{N_i}{q_{i,sat} Đ_i} \qquad (1)$$

The fractional occupancies are defined by:

$$\theta_i = \frac{q_i}{q_{i,sat}} \qquad (2)$$

In these equations:

$$\rho = density\ of\ the\ membrane\ \frac{Kg}{m^3}$$

$$Đ_i = M - S\ diffusivity\ of\ species\ i\ \frac{m^2}{s}$$

$$Đ_{i,j} = M - S\ diffusivity\ describing\ interchange\ between\ i\ and\ j\ \frac{m^2}{s}$$

$$N_i = molar\ flux\ of\ species\ i\ \frac{mol}{m^2 s}$$

$$\mu_i = molar\ chemical\ potential\ \ \frac{J}{mol}$$

As can be seen, there are two types of M-S diffusivities.

Diffusion in zeolites occurs by a molecular jump process. When the jump of species i creates a vacancy filled by species i, this is described by $Đ_i$, the diffusivities that reflect the interactions between species i and the zeolite. These diffusivities are referred to as jump or "corrected" diffusivities. When the vacancy is filled by species j, the process is described by $Đ_{i,j}$.

Diffusion in zeolites is an activated process, which can be represented (for gas transport) by:

$$Đ_i = \frac{\alpha}{z}\left(\frac{8RT}{\pi M}\right)^{\frac{1}{2}} \exp\left(\frac{-E_d}{RT}\right) \quad (3)$$

In this equation

$$\alpha = diffusion\ length$$

$$z = diffusion\ coordination\ number$$

$$M = molecular\ weight\ of\ i$$

$$E_d = activation\ energy\ for\ diffusion$$

However in applying the M-S model, the values for $Đ_i$ are measured and the values for $Đ_{i,j}$ are calculated by a logarithmic interpolation formula:

$$Đ_{i,j} = [Đ_i]^k [Đ_j]^l \quad (4)$$

where

$$k = \frac{-\theta_i}{\theta_i + \theta_j} \quad (5)$$

and

$$l = \frac{-\theta_j}{\theta_i + \theta_j} \quad (6)$$

Two types of experimental methods, microscopic and macroscopic have been applied to measure diffusion ($Đ_i$) in zeolites. [26, 27] Microscopic techniques include pulsed field gradient NMR and quasi-elastic neutron scattering Macroscopic techniques can be further divided into steady state and transient methods. Steady state methods include the Wicke-Kallenbach permeation method and the single crystal membrane technique. Transient techniques include chromatography, frequency response, zero-length column, and membrane transient permeation techniques.

The chemical potential gradients in equation (1) may be expressed in terms of the gradients of the occupancies by introduction of the matrix of thermodynamic factors [Γ]:

$$\frac{\theta_i}{RT}\frac{\delta \mu_i}{\delta z} = \sum_{j=1}^{n} \Gamma_{i,j}\frac{\delta \theta_j}{\delta z} \quad (7)$$

Where

$$\Gamma_{i,j} = \frac{\theta_i}{p_i}\frac{\delta p_i}{\delta \theta_j} \quad (8)$$

$$p_i = partial\ pressure\ of\ component\ i$$

The individual component loadings can be assumed to follow the multicomponent Langmuir isotherm:

$$\theta_i = \frac{b_i p_i}{1 + \sum_{i=1}^{n} b_i p_i} \quad (9)$$

$$b_i = parameter\ in\ the\ pure\ component\ Langmuir\ adsorption\ isotherm\ \ Pa^{-1}$$

Other adsorption isotherms may also be used, as described by Ruthven [27]. In brief they are:

1. At sufficiently low adsorbed phase concentrations on a homogenous surface, the isotherm should approach linearity (Henry's law). At higher loadings the following isotherms (Type 1 in Brunauer's classification) may be used:
2. The ideal Langmuir model
3. The dual-site Langmuir model (for energetically heterogeneous adsorbents)
4. The Unilan model.
5. The Toth model
6. The Simplified Statistical Model
7. The Gibbs Adsorption isotherm. This model represents an alternative approach to the other models. In this model, the adsorbed phase is regarded as a fluid held within the force field of the adsorbent, and is characterized by an equation of state. The Gibbs adsorption isotherm is written as:

$$\frac{\pi}{p} = (\frac{\delta\pi}{\delta p})_T \quad (10)$$

$$\pi[f(q,T)] = \text{spreading pressure}$$

8. The Dubinin-Polanyi theory
9. The ideal adsorbed solution theory (based on integration of the Gibbs isotherm)

An important consideration is that for most real systems there is a significant loading dependence on temperature. Adsorption is an exothermic process while vaporization is endothermic. This results in a temperature gradient across the zeolite membrane. Kuhn et al. [28] suggest that the M-S model should be modified to take the temperature gradient into account. In the system they studied, water flux across a NaA

zeolite membrane, a temperature gradient of 1.3 K was found. The also noted significant contribution of the support to mass transfer resistance.

The Maxwell-Stefan model can be very useful in predicting the fluxes of the feed mixture components, and the selectivity of the zeolite. A significant limitation in using this model is the difficulty in obtaining the input data (diffusivities and component loadings). Additionally, to analyze the zeolite layer in conjunction with the support requires coupling with a second model for flux through the support such as the dusty gas model.

1.3.3 **Mathematical Modeling of Transport in the Support Layer**

Flux through the support is a combination of Knudsen and viscous flow. Knudsen flow of a gas (i.e. permeate) occurs in a porous media such as a support when the mean free path of the gas is greater than the pore diameter. In Knudsen flow the gas molecules are more likely to hit the walls of the porous media than each other. The diffusion of gas species i and j may be regarded as independent of each other. Viscous flow of a gas occurs when the pore diameter is large, or in the absence of pores. In viscous flow, the flow is inversely rather than directly proportional to the viscosity. Knudsen flow predominates over viscous flow at low pressures since Knudsen flow is directly proportional to the pressure at the zeolite/support interface while viscous flow is directly proportional to the square of that pressure.

On a molecular level, viscosity is the product of the density, mean velocity, and mean free path of the gas. The product of the mean velocity and mean free path is known as the kinematic viscosity or "momentum diffusivity". In Newton's law of viscosity, the product of the density and the momentum diffusivity, the viscosity, is the proportionality

factor between the shearing force per unit area and its resultant velocity gradient. In an analogous way, the product of density and mass diffusivity is the proportionality factor between flux and the mass fraction gradient. Although momentum diffusivity and mass diffusivity have the same units ($\frac{m^2}{s}$), they differ in that shearing force per unit area is a tensor while the flux through a membrane is a vector directed perpendicular to the membrane surface [29]. The flux, mass transfer per area per second, of a permeating species through the composite membrane is identical through all its layers (conservation of mass).

Mathematical modeling of flux through the support has been done using the dusty gas model or a "pseudo binary diffusion" model. A simpler model has been proposed by de Bruijn [23]: This model uses the assumption of a single permeating species and the following flux equations for the support:

$$J_{Kn,i} = -\frac{1}{RT} D_{Kn,i}^{eff} \nabla p_i \qquad (11)$$

$$D_{Kn,i}^{eff} = \frac{\varepsilon}{\tau} \frac{d_0}{3} \sqrt{\frac{8RT}{\pi M_i}} \qquad (12)$$

$$J_{vis,i} = -\frac{p_{ave,i}}{RT} \frac{B_0^{eff}}{\eta} \nabla p_i \qquad (13)$$

$$B_0^{eff} = \frac{\varepsilon}{\tau} \frac{d_0^2}{32} \qquad (14)$$

Using this model requires the following input data:

1. Total flux through the composite zeolite-support membrane
2. Separation factor

3. Feed pressure of the permeating species
4. Permeate pressure of the permeating species
5. Pore diameter of the support
6. Thickness of the support
7. Viscosity of the permeating species
8. Temperature
9. Values for ε and τ (often estimates)

The molar flux of the permeating species is calculated using the total flux and the separation factor. Once the molar flux of the permeating species is determined then the equation:

$$J_{molar,i} = J_{Kn,i} + J_{vis,i} \quad (15)$$

has only one unknown, the zeolite-support interfacial pressure, which can then be readily calculated. Once this pressure is known, de Bruijn used

$$resistance\ to\ mass\ transfer = \frac{-\Delta p_{support,i}}{-\Delta p_{total,i}} \quad (16)$$

as an index of support resistance.

The de Bruijn study included a large retrospective review of the pervaporation literature. Pervaporation separations were broken down to two groups: dehydration of organics, and organics separations. Dehydration separations utilized a hydrophilic zeolite membrane while organic separations utilized an organophilic (hydrophobic) zeolite membrane. Fluxes and separation factors were high for the dehydration of organics and support resistance to mass transfer was found to be significant in that group. Fluxes and separation factors were significantly lower in the organic separations. However support

resistance to mass transfer was found to be significant for several cases within the second group, included ethanol separation from water using a silicalite-1 membrane. They also determined that Knudsen flow dominated over viscous flow in the support, well over 90% in systems where the flux was < 5 $\frac{kg}{m^2h}$, with pore diameters up to 5μ.

A significant limitation of the de Bruijn model is that it requires the input of support properties ε, τ, and pore diameter that may be difficult to obtain. 14 of 18 of the studies evaluated in the de Bruijn study were examined [19, 30-46]. Values for ε and τ were not provided in any of the 14. De Bruijn had to use estimates. Similarly, pore diameter of the support was usually not measured, the value provided by the industrial supplier of the support was often used. Another limitation is that the "resistance to mass transfer" does not provide how much flux was lost relative to the theoretical flux of the stand- alone zeolite layer. Also, an analysis of the relation of "resistance to mass transfer" to selectivity was not provided.

1.4 **RESEARCH MOTIVATION AND STRUCTURE OF THE THESIS**

Pervaporation, a membrane separation process, was described in the foregoing pages. A description of zeolites, and zeolite membranes used for pervaporation was provided. The use of the zeolite silicalite-1 in pervaporation was summarized. The results of research efforts investigating silicalite-1 for ethanol/water separation by pervaporation were shown in table 1.1. The fluxes and separation factors obtained were significantly less than those achieved by the NaA zeolite membrane used industrially for ethanol dehydration.

Mathematical models including the Maxwell-Stefan model and the de Bruijn et al. model were described as ways to evaluate zeolite supported membrane performance.

For example, the de Bruijn model suggests that flux is limited by the support in the pervaporation separation of ethanol from water using a supported silicalite-1 membrane. The limitations of the Maxwell-Stefan model and the de Bruijn model were discussed. These limitations, and the relatively poor performance of silicalite-1 for pervaporation separation of ethanol from water provided the motivation for this thesis.

Objectives of research:

1. To develop a mathematical model of a supported zeolite membrane that provides information about how much flux and selectivity is lost because of support resistance.
2. The model should require input data that are easy to obtain.
3. Show the effectiveness of the model using input values obtained experimentally and from the literature.

The remainder of this thesis will follow the structure:

1. Chapter 2 will present the model along with a graphical analysis
2. Chapter 3 will present the experiments done to evaluate the model and will apply the model to data from the literature
3. Chapter 4 will present a summary and recommendations
4. Appendices will show the mathematical derivations of the models

CHAPTER 2

THE FLUX AND SELECTIVITY MODEL

2.1 **BACKGROUND FOR THE MODEL**

2.1.1 **Introduction**

Several types of models for zeolite supported membranes in pervaporation were illustrated in the previous chapter. The Maxwell-Stefan model for transport through the zeolite layer coupled with a suitable model, such as the dusty gas model, for transport through the support was discussed. This type of model uses the assumptions of coupled binary diffusion through the zeolite layer and coupled Knudsen and viscous flow in the support to predict fluxes and selectivities. Models such as the Maxwell-Stefan model, are complex, often requiring a significant amount of difficult to obtain input data. The de Bruijn et al. model is different in that it is a model of support resistance. It assumes Knudsen and viscous flow through the support, assumes a single permeating species, and requires input of intrinsic support values of porosity and tortuosity. Although simpler to use then the Maxwell-Stefan model, the de Bruijn model is more descriptive than predictive. It uses the "ratio of mass transfer resistance" to define supports of zeolite supported membranes with high (dehydrations) and low (organic separations) resistance in pervaporation - the main conclusion of the de Bruijn study was that flux of the main permeating species was limited by support resistance, mainly in the case of high flux dehydration of organics, when using zeolite supported membranes in pervaporation.

The objective of this chapter is to establish simple predictive models for both flux and selectivity for a zeolite supported membrane in pervaporation. The simplicity of these models lay in part in the fact that the input data required are the results of Helium

permeance studies for the supports and the permeance values of both species for the zeolite layer obtained from a single pervaporation. The model equations do not use intrinsic support properties such as tortuosity or zeolite layer diffusivites and adsorptions. The flux model, in its simplest form, and the selectivity model assume 100% Knudsen flow through the support. The range of support pore sizes that are compatible with the synthesis of a zeolite layer, in general, produce predominantly Knudsen flow. Both the flux and selectivity models are based on the resistance in series model for zeolite supported membranes. The effect of temperature on the model equations will also be shown.

2.1.2 **Resistance in Series**

In an electrical series circuit, the total resistance is the sum of the individual resistances. Three axioms make this true: Ohm's law; the current is equal throughout the circuit; and the total voltage is the sum of the voltage drops across the resistors. The resistance in series model in membrane science analogously regards the layers of the membrane as a "circuit" so that the sum of the resistances of the individual membrane layers is equal to the total resistance of the membrane. The derivation below is given for a zeolite supported membrane used for pervaporation.

Following the resistance in series model for the electrical series circuit, the "current" in a membrane system is flux of a species, everywhere equal; and the "voltage" is the pressure drop of the species across the membrane layers (driving force) where the total pressure drop is the sum of the individual pressure drops. By Ohm's law:

$$Resistance = \frac{pressure\ drop}{flux} \qquad (17)$$

where

$$pressure\ drop = -\Delta p_{layer,i}$$

$$flux, i = J_{molar,i}$$

Defining the pressure drops of the membrane layers:

$$-\Delta p_{support,i} = p_{interface,i} - p_{permeate,i} \quad (18)$$

$$-\Delta p_{zeolite,i} = p_{feed,i} - p_{interface,i} \quad (19)$$

$$-\Delta p_{total,i} = p_{feed,i} - p_{permeate,i} \quad (20)$$

$$p_{permeate,i} = permeate\ pressure\ of\ \ i$$

$$p_{interface,i} = pressure\ of\ \ i\ at\ the\ zeolite/support\ interface$$

$$p_{feed,i} = feed\ pressure\ of\ \ i$$

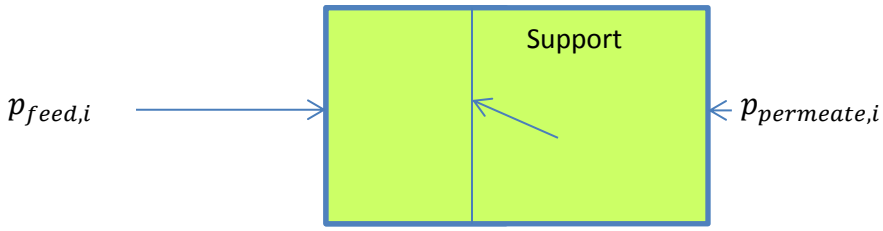

Figure 2.1

Pressures of a permeating species across a zeolite supported membrane in pervaporation

In figure 2.1 the feed is a liquid. $p_{feed,i}$ $(y_i p)$ is obtained using the following relationship:

$$y_i p = x_i \gamma_i p_i^{sat} \quad (21)$$

Where

$$y_i p = partial\ pressure\ of\ i, feed$$

$$x_i = liquid\ mole\ fraction, i$$

$$\gamma_i = activity\ coefficient\ of\ i\ (from\ Van\ Laar\ equation)$$

$$p_i^{sat} = saturation\ pressure\ of\ i\ (from\ Antoine\ equation)$$

The value of $p_{interface,i}$ is the pressure of species "i" at the zeolite/support interface. It is a calculated value obtained from the support permeance of "i"and the molar flux of "i", as described below. The permeate pressure, $p_{permeate,i}$ can be calculated if the permeate composition is known and if the total permeate pressure is known. In pervaporation, the permeate side is set to a vacuum so that a reasonable assumption is to set the permeate pressure to zero, as will be done here. Consequently

$$Resistance, support\ layer, i = \frac{p_{interface,i} - p_{permeate,i}}{J_{molar,i}} \quad (22)$$

$$Resistance, zeolite\ layer, i = \frac{p_{feed,i} - p_{interface,i}}{J_{i,molar}} \quad (23)$$

$$Resistance, total, i = \frac{p_{feed,i} - p_{permeate,i}}{J_{molar,i}} \quad (24)$$

It was stated in chapter 1 that pressure drop across a membrane layer is the driving force to produce flux. It can be seen from equation (17) that to keep resistance low, pressure drop should be small, and flux should be large. That is, the most desirable case is for a small pressure drop to produce a large flux. It can also be seen from equations (22) and (23) that the critical pressure parameter, $p_{interface,i}$ influences both the resistance of the support and the resistance of the zeolite layer. However, because the feed pressure is usually much larger than the interfacial pressure or the permeate pressure, the interfacial pressure influences support resistance more than zeolite

resistance. The underlying premise for the model to be developed here, and for zeolite supported membrane pervaporation performance in general, is that support resistance should be kept to a minimum for the main permeating species.

The resistance in series model states, for a species:

$$Resistance, i, total = Resistance, i, zeolite\ layer + Resistance, i, support\ layer \quad (25)$$

Substituting equations (22 , 23, and 24) into equation (25):

$$\frac{p_{feed,i} - p_{permeate,i}}{J_{molar,i}} = \frac{p_{feed,i} - p_{interface,i}}{J_{molar,i}} + \frac{p_{interface,i} - p_{permeate,i}}{J_{molar,i}} \quad (26)$$

Then multiplying equation (24) by $J_{i,molar}$ results in:

$$p_{feed,i} - p_{permeate,i} = p_{feed,i} - p_{interface,i} + p_{interface,i} - p_{permeate,i} \quad (27)$$

Equation (27) shows that the above definitions of resistance and pressure drop for a zeolite supported membrane satisfy the three axioms of the resistance in series model.

Permeance for a species is defined as:

$$Permeance = \frac{flux}{pressure\ drop} \quad (28)$$

$$Permeance, layer, i = F_{layer,i}$$

$$F_{layer,i} = \frac{J_{molar,i}}{-\Delta p_{layer,i}} \quad (29)$$

Therefore permeance is the reciprocal of resistance. Inserting this relationship into equation (25) results in:

$$\frac{1}{Permeance, i, total} = \frac{1}{Permeance, i, zeolite} + \frac{1}{Permeance, i, support} \quad (30)$$

Or:

$$\frac{1}{F_{total,i}} = \frac{1}{F_{zeolite,i}} + \frac{1}{F_{support,i}} \quad (31)$$

2.1.3 **Resistance Ratio of Support to Zeolite**

The model will construct dimensionless groups from the ratios of the permeances of the membrane layers. Because of the reciprocal relationship between resistance and permeance, these dimensionless groups are resistance ratios. For a single pervaporation, the molar flux terms in the numerator and denominator of the resistance ratios cancel producing mathematically equivalent ratios of the pressure drops required to produce the flux. Given the condition of a single pervaporation, the resistance ratios and the model equations can then be reformulated in terms of ratios of the pressure drops required to produce the flux obtained from that single pervaporation. The purpose of that reformulation is to provide a more intuitive understanding of the physical meaning of the model equations, and to provide a basis for comparison to the de Bruijn et al. model.

The first dimensionless group is "resistance ratio of support to zeolite." The resistance ratio of support to zeolite is obtained starting with the following expression for support permeance:

$$F_{support,i} = \alpha_i + (\beta p_{ave})_i \quad (32)$$

$$\alpha_i = Knudsen\ permeance\ of\ i, support$$

$$(\beta p_{ave})_i = viscous\ permeance\ of\ i, support$$

Using equation (28) and equation (32) results in the following expression for flux through the support:

$$J_{molar,i} = (\alpha_i + (\beta p_{ave})_i)(-\Delta p_{support,i}) \quad (33)$$

Comparison of equation (33) with equations (11, 13, and 15) shows that

$$J_{Kn,i} = \alpha_i\left(-\Delta p_{support,i}\right) \quad (34)$$

$$\alpha_i = \frac{1}{\sqrt{RT}}\frac{\varepsilon}{\tau}\frac{d_0}{3L}\sqrt{\frac{8}{\pi M_i}} \quad (35)$$

And

$$J_{vis,i} = (\beta p_{ave})_i(-\Delta p_{support,i}) \quad (36)$$

The definition of the resistance ratio of support to zeolite is based on the assumption of only Knudsen flow through the support. This assumption is valid under the conditions of low pressure and small pore diameter. As already stated, this assumption is reasonable in many zeolite supported membranes where fluxes < 5 $\frac{Kg}{m^2 hr}$ are generated by pervaporation [23]. If 100% Knudsen flow is assumed, equation (33) becomes:

$$J_{molar,i} = \alpha_i\left(-\Delta p_{support,i}\right) \quad (37)$$

Then

$$\alpha_i = \frac{J_{molar,i}}{-\Delta p_{support,i}} \quad (38)$$

The permeance of the zeolite layer is:

$$F_{zeolite,i} = \frac{J_{molar,i}}{-\Delta p_{zeolite,i}} \quad (39)$$

And the resistance ratio of support to zeolite, species "i" is defined as:

$$resistance\ ratio\ of\ support\ to\ zeolite, i = \frac{F_{zeolite,i}}{\alpha_i} \quad (40)$$

Or, using the reciprocal relationship between permeance and resistance,

$$resistance\ ratio\ of\ support\ to\ zeolite, i = \frac{resistance\ of\ support, i}{resistance\ of\ zeolite\ layer, i} \quad (41)$$

When the molar flux terms in equations (38) and (39) are identical, equations (38) and (39) can be substituted into equation (40):

$$resistance\ ratio\ of\ support\ to\ zeolite, i = \frac{-\Delta p_{support,i}}{-\Delta p_{zeolite,i}} \quad (42)$$

Equation (42) is valid when the molar flux terms in equations (38) and (39) are identical, and therefore can be dropped from the numerator and denominator of the RHS of equation (40). When the model equations are used to predict the results of a second prevaporation, equation (40) must be used, not equation (42). Both the numerator and denominator of the RHS of equation (42) represent the pressure drops required to produce the flux of a single pervaporation across the membrane layers. High pressure drop as a driving force and low pressure drop per unit of flux (resistance) are both desirable. The resistance ratio is assigned the following variable designation:

$$resistance\ ratio\ of\ support\ to\ zeolite, i = \phi_i$$

2.1.4 **Temperature Dependence Of The Resistance Ratio Of Support To Zeolite** $(\boldsymbol{\phi_i})$

The first step to obtain the temperature dependence of the resistance ratio of support to zeolite is to modify equation (40) to show temperature dependency:

$$\phi_{i,T} = \frac{F_{zeolite,i,T}}{\alpha_{i,T}} \quad (43)$$

The temperature dependence of $F_{zeolite,i}$ is evaluated (a simplifying assumption of a single permeating species is made) [10]:

$$F_{zeolite,i} = K_{z2}\sqrt{\frac{1}{RTMw_i}}\exp\left(\frac{-E_{d,i}}{RT}\right) \quad (44)$$

$$K_{z2} = constant, containing\ \varepsilon, \tau, L, and\ adsorption\ equilibrium\ constant$$

$$E_{d,i} = activated\ energy\ of\ diffusion, i\ (\frac{KJ}{mol})$$

Equation (44) can be compared with equation (39). Equation (38) obtains $F_{z,i}$ from quantities that are extrinsic to the membrane. Equation (44) obtains $F_{z,i}$ from quantities that are intrinsic to the membrane. Equation (44) allows an evaluation of temperature dependency.

$$F_{zeolite,i,T_2} = \sqrt{\frac{T_1}{T_2}} \exp\left(\frac{E_{d,i}}{R}\left(\frac{1}{T_1} - \frac{1}{T_2}\right)\right) F_{zeolite,i,T_1} \quad (45)$$

The temperature dependence of α_i is evaluated:

$$\alpha_i = -\frac{1}{\sqrt{RT}} \frac{\varepsilon}{\tau} \frac{d_0}{3L} \sqrt{\frac{8}{\pi M_i}} \quad (35)$$

Therefore:

$$\alpha_{i,T_2} = \sqrt{\frac{T_1}{T_2}} \alpha_{i,T_1} \quad (46)$$

Substituting equations (45) and (46) into equation (43) results in:

$$\phi_{i,T_2} = \exp\left(\frac{E_{d,i}}{R}\left(\frac{1}{T_1} - \frac{1}{T_2}\right)\right) \phi_{i,T_1} \quad (47)$$

If ϕ_{i,T_1} represents ethanol at 298 K, the following plot of equation (47) is obtained:

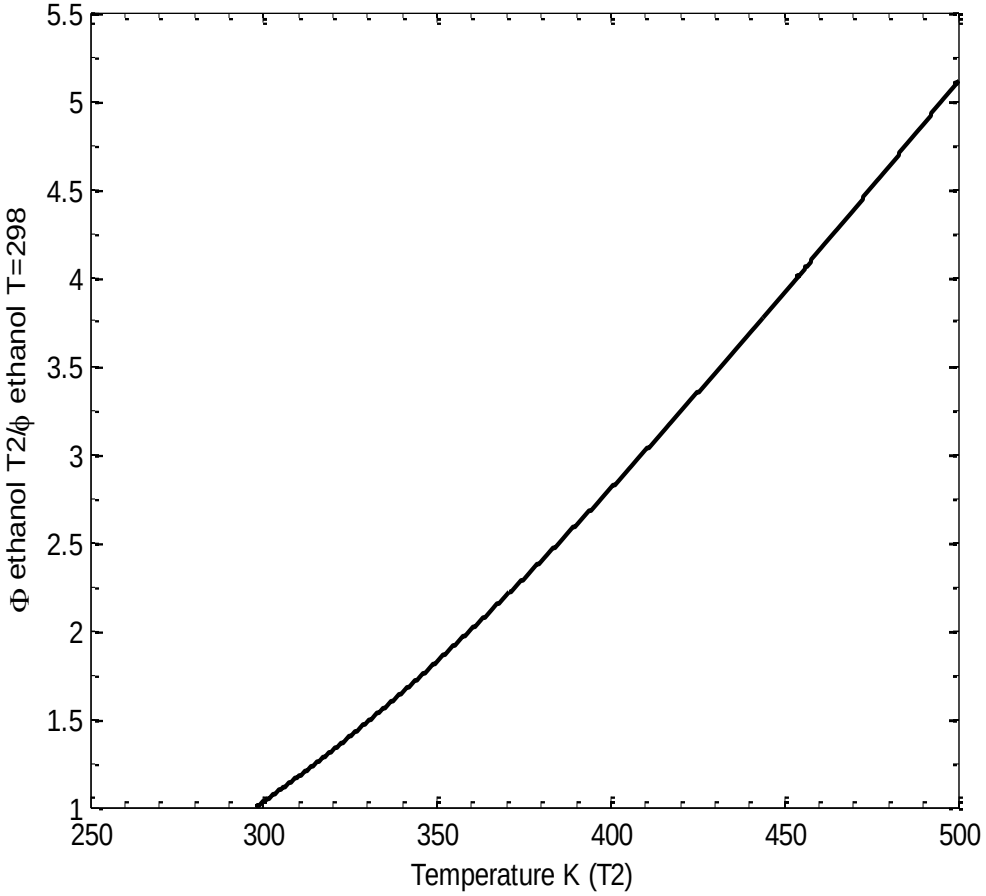

Figure 2.2

Temperature dependence of ϕ_i for ethanol $\frac{E_{d,i}}{R}$ =1202.8 K (estimate [47])

Figure 2.2 shows that the ratio $\frac{\phi_{i,T2}}{\phi_{i,298}}$ increases exponentially with the difference in the reciprocals of temperature, $\frac{1}{298} - \frac{1}{T_2}$. Therefore ϕ_i increases with increasing temperature.

2.2 **THE FLUX MODEL**

2.2.1 **Relative Permeation Flux**

With equation (32) the molar flux of species "i" is obtained by multiplying the support permeance by the pressure drop across the support.

$$J_{molar,i} = (\alpha_i + (\beta p_{ave})_i)(-\Delta p_{support,i}) \quad (33)$$

Similarly, the molar flux of species "i" can be obtained by multiplying the zeolite permeance by the pressure drop across the zeolite layer:

$$J_{molar,i} = F_{zeolite,i}(-\Delta p_{zeolite,i}) \quad (48)$$

Ideal flux for species "i" is defined as:

$$J_i^o = ideal\ flux\ through\ the\ zeolite\ layer, no\ support, permeate\ pressure = 0$$

$$J_i^o = F_{zeolite,i}(p_{feed,i}) \qquad (49)$$

The RHS of equation (33) can be equated to the RHS of equation (48). A solution for $p_{interface,i}$ is obtained and inserted into equation (48)

The following dimensionless groups are defined:

$$\Pi_i = \frac{J_{molar,i}}{J_i^o}, relative\ permeation\ flux, i \quad (50)$$

$$\Gamma_i = \frac{\beta x_i \gamma_i p_i^{sat}}{\alpha_i} \qquad relative\ importance\ of\ the\ support\ pore\ size, i \quad (51)$$

A rough estimate of the ratio of viscous flow to Knudsen flow in the support is provided by Γ_i (see appendix A).

By dividing equation (48), after substitution for $p_{interface,i}$, by equation (49), and substituting the dimensionless groups as defined above, the flux model equation is obtained:

$$\Pi_i = 1 - \frac{1}{\Gamma_i}\{[\left(1 + \phi_i)^2 + 2\phi_i\Gamma_i\right]^{\frac{1}{2}} - (1 + \phi_i)\} \quad (52)$$

The flux model equation (54) has the ratio of real to ideal flux, relative permeation flux, Π_i, as a function of two other dimensionless groups, ϕ_i and Γ_i.

Equation (52) is displayed graphically:

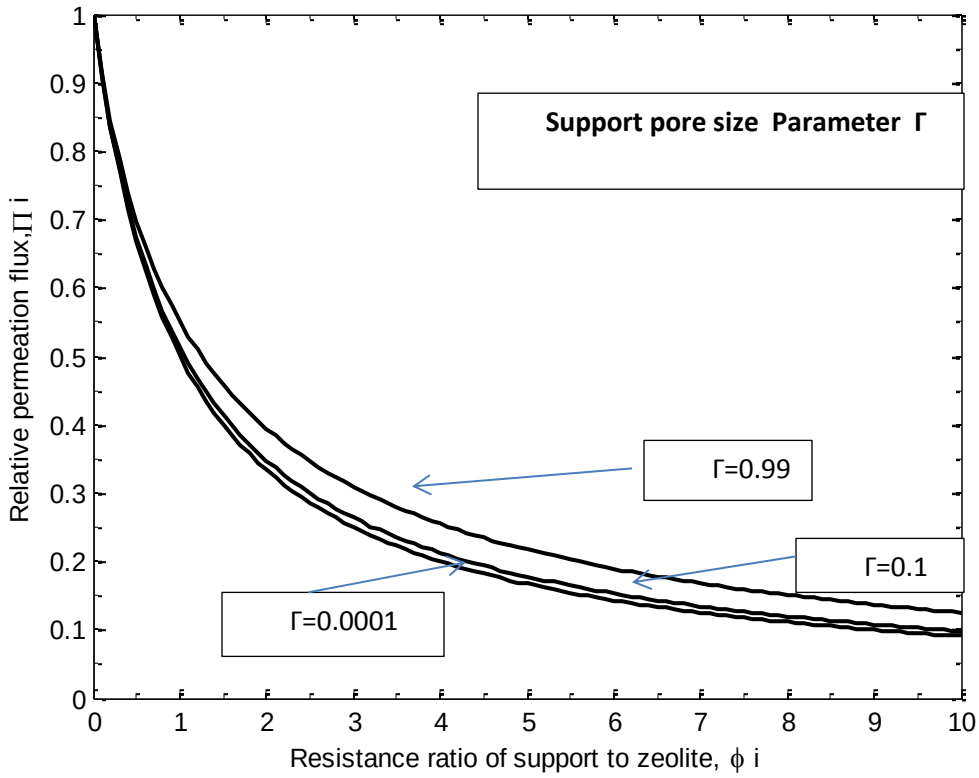

Figure 2.3

Relative permeation flux as a function of the resistance ratio of support to zeolte at different representative Γ_i values

Figure 2.3 shows the effects of the resistance of the support on the pervaporation relative permeation flux through the zeolite membranes. The larger the resistance, the more reduction in relative permeation flux. Starting from the flux of the membrane without support (zero relative resistance), the increase in the resistance of the support has dramatic effect in reduction in permeation flux. For example, when the resistance of the support is about the same as that of zeolite, the permeation flux is reduced by about 50%.

Further increase in the support resistance has less effect on reduction in relative permeation flux. The pore size of the support has some effect on permeation flux, but the effects are minor to the relative resistance of the support (porosity and thickness).

As can be seen from Figure 2.3 if there is less than 10-20% viscous flow in the support ($\Gamma_i < 0.1$), the value of Γ_i will produce virtually identical curves of Π_i vs. ϕ_i.

It is therefore useful to obtain an alternate expression for Π_i under the common circumstance of negligible viscous flow in the support (β=0). This is obtained in the same way equation (52) is obtained, except that initially equation (37) is used in place of equation (33). The result is:

$$\Pi_i = \frac{1}{1 + \phi_i} \quad (53)$$

Equation (53) can also be obtained from equation (52) by taking the limit $\Gamma_i \rightarrow 0$, using L'Hospital's law.

Equation (53) is displayed graphically:

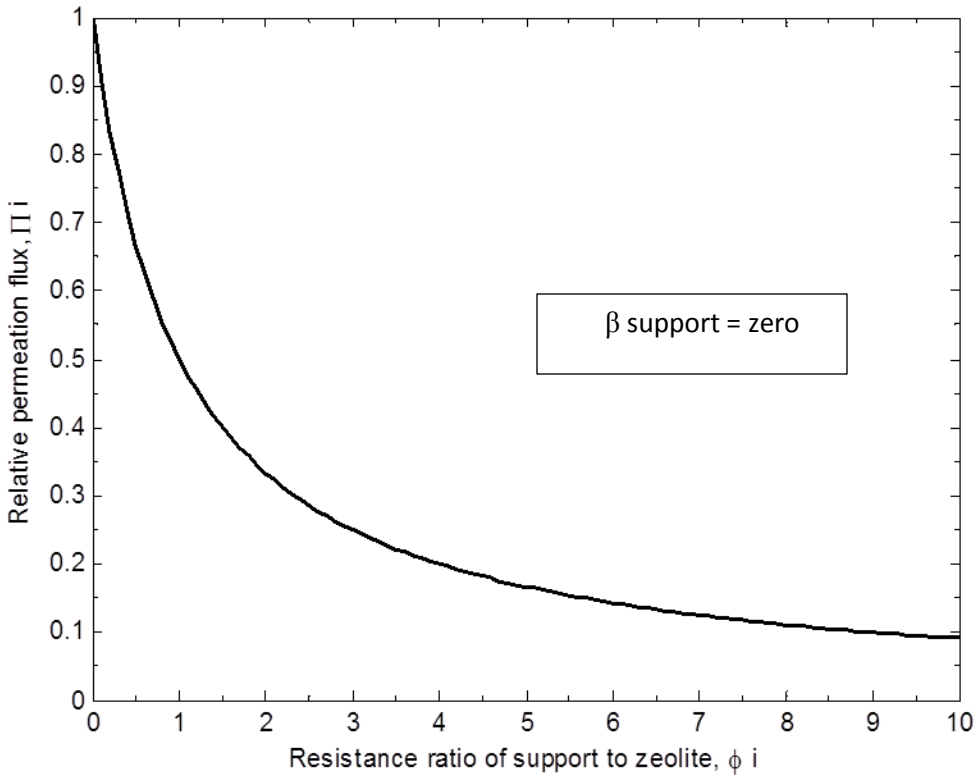

Figure 2.4

Relative permeation flux as a function of the resistance ratio of support to zeolite, $\beta\ support = 0$

The curve in Figure 2.4 represents the lowest curve of all possible curves that could have been presented in Figure 2.3

It is also possible to express Π_i in terms of ratios of pressure drops:

$$\Pi_i = \frac{J_{molar,i}}{J_i^o} \qquad (50)$$

$$J_i^o = F_{zeolite,i}(p_{feed,i}) \qquad (49)$$

$$F_{zeolite,i} = \frac{J_{molar,i}}{-\Delta p_{zeolite,i}} \qquad (39)$$

Equation (38) and be substituted into equation (48), and the resultant equation substituted into equation (49) to get:

$$\Pi_i = \frac{J_{molar,i}}{\frac{J_{molar,i}(p_{feed,i})}{-\Delta p_{zeolite,i}}} \quad (54)$$

or:

$$\Pi_i = \frac{-\Delta p_{zeolite,i}}{(p_{feed,i})} \quad (55)$$

Equation (55) is valid when the molar flux terms in the numerator and denominator of equation (54) are identical. Under that circumstance:

$$\Pi_i = resistance\ ratio\ of\ zeolite\ to\ total, i$$

This definition is valid only under the stated conditions.

Equations (42) and (55) may be substituted into equation (53) to get:

$$\frac{-\Delta p_{zeolite,i}}{(p_{feed,i})} = \frac{1}{1 + \frac{-\Delta p_{support,i}}{-\Delta p_{zeolite,i}}} \quad (56)$$

Note that equations (55) and (56) are valid only when the molar flux terms in the numerator and denominator of equations (40) and (54) are identical. Equation (56) can easily be rearranged to produce equation (26) or equation (27) and therefore is a form of the resistance in series equation. Since equation (53) is directly obtainable from equation (56) it also is a form of the resistance in series equation.

In terms of the resistance in series model, equation (56) relates the ratio of "currents" (Π_i), as the resistance ratio of zeolite to total, to the resistance ratio of support to zeolite. Examination of equations (52), (53), and (56) show that the maximum value

of Π_i, 1, is approached as support resistance approaches zero. When support resistance approaches zero, the flux of the total membrane approaches the ideal flux of the zeolite layer; the resistance of the total membrane approaches the resistance of the zeolite layer. Since there is always a support, there is always support resistance. The goal is to keep support resistance for the main permeating species to a minimum.

2.2.2 **Temperature Dependence of Relative Permeation Flux**

To show the effect of temperature on flux, equation (52) is modified to show temperature dependence:

$$\Pi_{i,T} = 1 - \frac{1}{\Gamma_{i,T}}\{[\left(1 + \phi_{i,T})^2 + 2\phi_{i,T}\Gamma_{i,T}\right]^{\frac{1}{2}} - \left(1 + \phi_{i,T}\right)\} \quad (57)$$

The temperature dependence of ϕ_i has been shown as:

$$\phi_{i,T_2} = \exp\left(\frac{E_{d,i}}{R}\left(\frac{1}{T_1} - \frac{1}{T_2}\right)\right)\phi_{i,T_1} \quad (47)$$

Equation (51) is modified to show temperature dependence:

$$\Gamma_{i,T} = \frac{\beta_T(x_i\gamma_i p_i^{sat})_T}{\alpha_{i,T}} \quad (58)$$

Comparing equation (13) and equation (33) shows that:

$$\beta = \frac{B_0^{eff}}{RTL\eta} \quad (59)$$

It will be assumed that viscosity is constant over the range of temperatures considered. This is necessary because there is no readily obtainable formula for the temperature dependence of viscosity at the relevant temperatures and pressures. The viscosity is obtained by analysis of empirical plots such as Fig. 1.3-1 from Transport Phenomena. The pressures of the permeating species in the support during pervaporation are usually

well below 5 kPa, so that the "low density limit" in Fig. 1.3-1 would be used to obtain the viscosity of a permeating species.

Therefore:

$$\beta_{i,T2} = \frac{T_1}{T_2}\beta_{i,T1} \quad (60)$$

The temperature dependence of $x_i\gamma_i p_i^{sat}$:

The mole fraction and activity coefficient (as determined by the Van Laar equation) are not temperature dependent. From the Antoine equation the temperature dependence of p_i^{sat} is:

$$p_{i,T_2}^{sat} = \exp\left(\left(\frac{B}{T_1 + C}\right) - \left(\frac{B}{T_2 + C}\right)\right) p_{i,T_1}^{sat} \quad (61)$$

The temperature dependence of α_i is:

$$\alpha_{i,T_2} = \sqrt{\frac{T_1}{T_2}}\alpha_{i,T_1} \quad (46)$$

Therefore:

$$\Gamma_{i,T_2} = \sqrt{\frac{T_1}{T_2}}\exp\left(\left(\frac{B}{T_1 + C}\right) - \left(\frac{B}{T_2 + C}\right)\right)\Gamma_{i,T_1} \quad (62)$$

And:

$$\Pi_{i,T_2} = 1 - \frac{1}{\sqrt{\frac{T_1}{T_2}}\exp(\left(\frac{B}{T_1 + C}\right) - \left(\frac{B}{T_2 + C}\right))\Gamma_{i,T_1}}\{[(1 + \exp\left(\frac{E_{d,i}}{R}\left(\frac{1}{T_1} - \frac{1}{T_2}\right)\right)\phi_{i,T_1}$$

$$)^2 + 2\sqrt{\frac{T_1}{T_2}}\exp(\left(\frac{B}{T_1 + C}\right) - \left(\frac{B}{T_2 + C}\right))\Gamma_{i,T_1}\exp\left(\frac{E_{d,i}}{R}\left(\frac{1}{T_1} - \frac{1}{T_2}\right)\right)\phi_{i,T_1}$$

$$]^{\frac{1}{2}} - \left(1 + \exp\left(\frac{E_{d,i}}{R}\left(\frac{1}{T_1} - \frac{1}{T_2}\right)\right)\phi_{i,T_1}\right)]\} \quad (63)$$

A representative plot of equation (63) with ϕ_{i,T_1} and Γ_{i,T_1} for ethanol, with $\frac{E_{d,i}}{R} = 1202.8\ K$ at 298 K is shown in Figure 2.5.

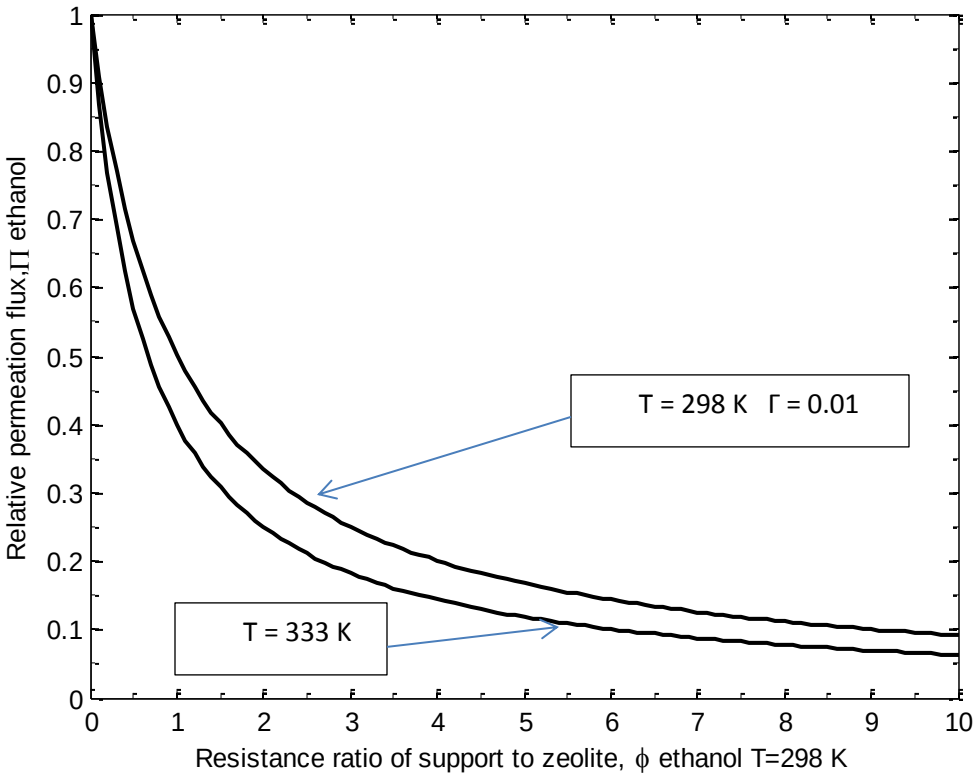

Figure 2.5

Effect of temperature on relative permeation flux

Figure 2.5 demonstrates that the effect of the resistance ratio of support to zeolite on relative permeation flux increases with increasing temperature. The effect of temperature on $\phi_{ethanol}$ has already been shown (Fig 2.2). A given value of $\phi_{ethanol}$ at T=298 K will result in a higher value of relative permeation flux at 298 K than at 333 K. For example, when $\phi_{ethanol}$ at T=298 K is equal to 2, the relative permeation is about 0.35. When the temperature is increased to 333 K, it can be seen, from figure 2.2 that $\phi_{ethanol}$ increases to about 3, and, from figure 2.5 that the relative permeation flux

decreases to about 0.25. Experimentally, flux increases with increasing temperature. Thus, the increase in ideal flux with increasing temperature is greater than the increase in real flux. This effect is more pronounced at lower values of the resistance ratio of support to zeolite.

The temperature dependence of Π_i when β=0 is readily obtained: In this case

$$\Pi_i = \frac{1}{1 + \phi_i} \quad (53)$$

Then equation (47) is applied:

$$\phi_{i,T_2} = \exp\left(\frac{E_{d,i}}{R}\left(\frac{1}{T_1} - \frac{1}{T_2}\right)\right)\phi_{i,T_1} \quad (47)$$

So therefore:

$$\Pi_{i,T2} = \frac{1}{1 + \exp\left(\frac{E_{d,i}}{R}\left(\frac{1}{T_1} - \frac{1}{T_2}\right)\right)\phi_{i,T_1}} \quad (64)$$

A representative plot of equation (64) with ϕ_{i,T_1} for ethanol at 298 K is shown in Figure 2.6:

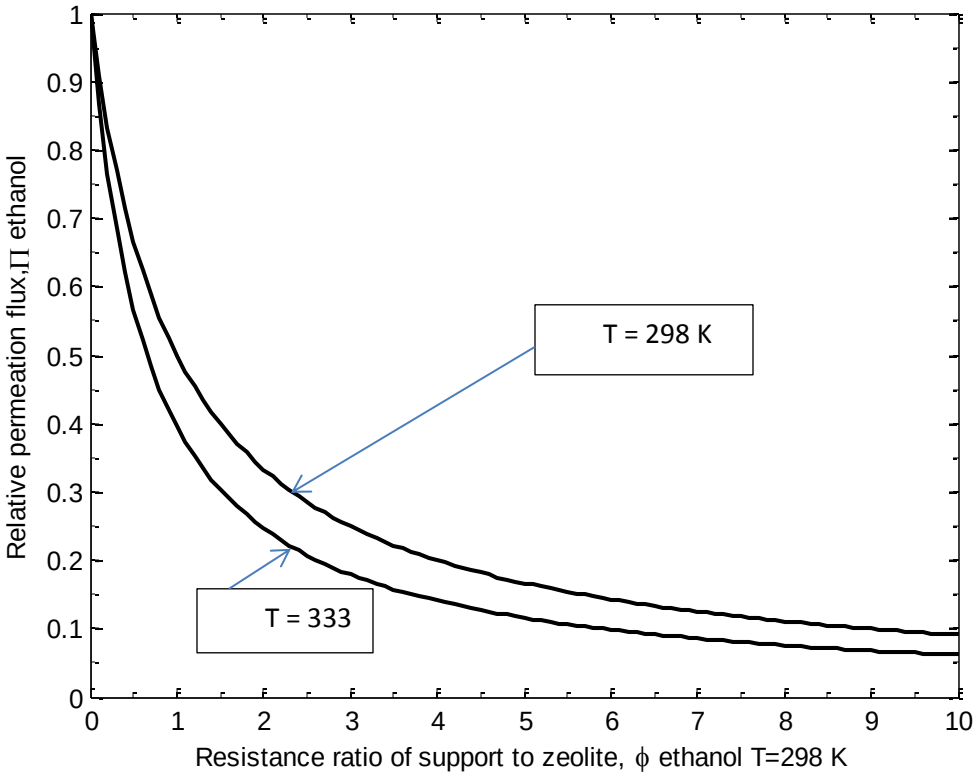

Figure 2.6

Effect of temperature on relative permeation flux, β=0

Figure 2.6 demonstrates that the effect of the resistance ratio of support to zeolite on relative permeation flux increases with increasing temperature. This effect is more pronounced at lower values of the resistance ratio of support to zeolite. The curve at T = 298 K is identical to the curve in figure 2.4. Both flux equations (with and without viscous flow in the support) show a similar temperature dependency.

2.3 **THE SELECTIVITY MODEL**

2.3.1 **Reduced Selectivity**

The selectivity portion of the model assumes 100% Knudsen flow (i.e. $\beta = 0$) through the support, in addition to $p_{p,i} = 0$. The derivation of this portion of the model is based on the resistance in series equation:

$$\frac{1}{F_{total,i}} = \frac{1}{F_{zeolite,i}} + \frac{1}{F_{support,i}} \quad (31)$$

The equation for molar flux through the zeolite layer is:

$$J_{molar,i} = F_{zeolite,i}\left(p_{feed,i} - p_{interface,i}\right) \quad (65) \quad (see\ eq. 51)$$

The equation for molar flux through the support, with $\beta = 0$ and $p_{p,i} = 0$ is:

$$J_{molar,i} = \alpha_i p_{interface,i} \quad (66) \quad (see\ eq. 36)$$

The total permeance of component "i" is given by

$$\frac{J_{molar,i}}{p_{feed,i}} = F_{total,i} \quad (67)$$

Combining equations (65), (66) and (67) results in:

$$F_{total,i} = F_{zeolite,i}\left(\frac{\alpha_i}{\alpha_i + F_{zeolite,i}}\right) \quad (68)$$

Equation (68) can be rearranged:

$$\frac{1}{F_{total,i}} = \frac{1}{\alpha_i} + \frac{1}{F_{zeolite,i}} \quad (31) \quad resistance\ in\ series$$

It follows from equation (68):

$$F_{total,j} = F_{z,j}\left(\frac{\alpha_j}{\alpha_j + F_{zeolite,j}}\right) \quad (69)$$

The selectivity model uses the following dimensionless groups:

$$S_{i,j} = \frac{F_{total,i}}{F_{total,j}} \qquad total\ selectivity \quad (70)$$

$$\frac{F_{zeolite,i}}{F_{zeolite,j}} = S_z \quad selectivity\ of\ zeolite\ membrane \quad (71)$$

$$S_s = \frac{\alpha_i}{\alpha_j} \qquad selectivity\ of\ support \quad (72)$$

$$\frac{\alpha_i}{\alpha_j} = \sqrt{\frac{Mw_j}{Mw_i}} \quad (73)$$

$$\phi_i = \frac{F_{z,i}}{\alpha_i} \quad (40)$$

$$Ln\ (Lin\ number) = \frac{S_s}{S_z} \quad (74)$$

Combining equations (68,69, and 70) and substituting equations (40, 71, 72, and 74) results in the selectivity model equation (see Appendix A):

$$\frac{S_{i,j}}{S_z} = \frac{1 + Ln\phi_i}{1 + \phi_i} \quad (75)$$

$$\frac{S_{i,j}}{S_z} = reduced\ selectivity$$

In the selectivity model equation, $\frac{S_{i,j}}{S_z}$, a dimensionless group, is a function of two dimensionless groups: Ln and ϕ_i. Equation (75) is shown graphically in Figure 2.7:

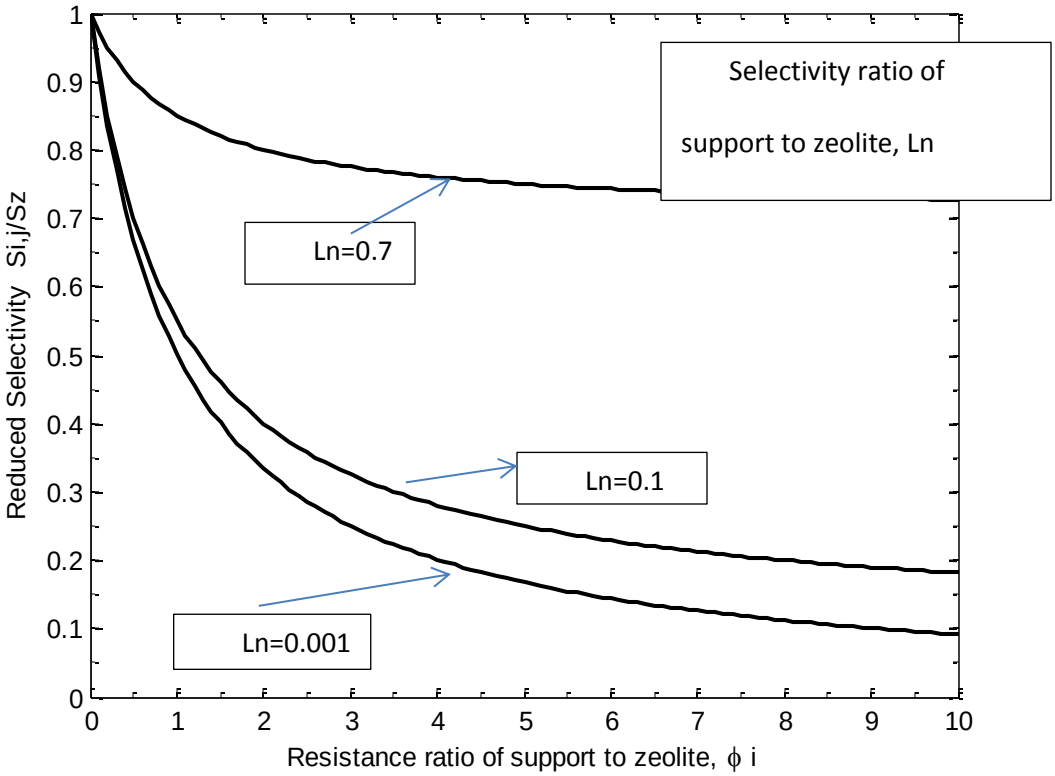

Figure 2.7

Reduced selectivity as a function of the resistance ratio of support to zeolite at different representative Ln values.

Figure 2.7 shows the effects of the support resistance on reduced selectivity of . As you see, reduced selectivity initially decreases dramatically with increasing support resistance. The effects depends on the selectivity of the support. The general trend is that as the support resistance increases the selectivity, $S_{i,j}$, decreases and becomes the same as that for the support. Mathematically, by L'Hospital's rule, the limit of $\frac{S_{i,j}}{S_z}$ as $\phi_i \rightarrow \infty$ is the Lin number, $\frac{S_s}{S_z}$. Since the support is usually macroporous with selectivity determined by Knudsen diffusion selectivity, the total membrane selectivity can drop

significantly and approaches to the Knudsen selectivity if the zeolite membrane is prepared on the support with resistance several times that of the zeolite layer. The Lin number has a significant effect on reduced selectivity.

It may be observed that:

$$Ln\phi_i = \phi_j \quad (76) \; resistance\; ratio\; of\; support\; to\; zeolite, j$$

So

$$\frac{S_{i,j}}{S_z} = \frac{1+\phi_j}{1+\phi_i} \quad (77)$$

$$\frac{S_{i,j}}{S_z} = \frac{\Pi_i}{\Pi_j} \quad (78)$$

Equation (75) can be expressed in terms of ratios of pressure drops with a similar method used to obtain equations (42) and (56), the assumption that the molar flux terms in the numerator and denominator of reduced selectivity, Lin number, and ϕ_i cancel. The following results are obtained:

$$Ln\phi_i = \frac{(-\Delta p_{support,j})}{(-\Delta p_{zeolite,j})} \quad (79)$$

$$\frac{\Pi_i}{\Pi_j} = \frac{1+\frac{(-\Delta p_{support,j})}{(-\Delta p_{zeolite,j})}}{1+\frac{-\Delta p_{support,i}}{-\Delta p_{zeolite,i}}} \quad (80) \; (see\; eq. 56)$$

$$\frac{\Pi_i}{\Pi_j} = \frac{(resistance\; ratio\; of\; zeolite\; to\; total)_i}{(resistance\; ratio\; of\; zeolite\; to\; total)_j} \quad (81)$$

Equation (77) is equation (53) used twice; for species "i" and for species "j", i.e. equation (53) for species "i" divided by equation (53) for species "j". Therefore equation (77), like equation (75) is a form of the resistance in series equation.

The maximum value of reduced selectivity, 1, is approached when support resistance approaches zero. As support resistance approaches zero, the selectivity of the overall membrane approaches the selectivity of the zeolite layer. As previously stated, the goal is to keep support resistance for the main permeating component, species "i", as close to zero as possible so that Π_i is as close to one as possible. On the other hand, the goal for species "j" is to obtain large support resistance and a value of Π_j as small as possible. Π_i is always less than Π_j since the ratio of real fluxes (i/j) is always less than the ratio of ideal fluxes (i/j).

2.3.2 **Temperature Dependence of Reduced Selectivity**

The derivation starts with the following equations:

$$F_{z,i,T_2} = \sqrt{\frac{T_1}{T_2}} \exp\left(\frac{E_{d,i}}{R}\left(\frac{1}{T_1} - \frac{1}{T_2}\right)\right) F_{z,i,T_1} \quad (44)$$

$$\alpha_{i,T_2} = \sqrt{\frac{T_1}{T_2}}\, \alpha_{i,T_1} \quad (45)$$

First

$$S_s = \frac{\alpha_i}{\alpha_j} \quad (72)$$

Therefore:

$$S_{sT_2} = S_{sT_1} \quad (82)$$

For S_z:

$$S_{z,T} = \frac{F_{z,i,T}}{F_{z,j,T}} \quad (83)$$

Substituting equation (44) for both i and j into equation (83) results in:

$$S_{z,T_2} = \exp\left(\left(\frac{E_{d,i} - E_{d,j}}{R}\right)\left(\frac{1}{T_1} - \frac{1}{T_2}\right)\right) S_{z,T_1} \quad (84)$$

$$\phi_{i,T_2} = \exp\left(\frac{E_{d,i}}{R}\left(\frac{1}{T_1} - \frac{1}{T_2}\right)\right)\phi_{i,T_1} \quad (46)$$

For the Ln number:

$$Ln_T = \frac{S_{s,T}}{S_{z,T}} \quad (85)$$

Substituting equations (82) and (84) into equation (85) results in:

$$Ln_{T_2} = \frac{S_{sT_2}}{S_{z,T_2}} = \frac{1}{\exp\left(\left(\frac{E_{d,i} - E_{d,j}}{R}\right)\left(\frac{1}{T_1} - \frac{1}{T_2}\right)\right)} Ln_{T_1} \quad (86)$$

Then combining equations (46) and (86) results in:

$$Ln_{T_2}\phi_{i,T_2} = \exp\left(\left(\frac{E_{d,j}}{R}\right)\left(\frac{1}{T_1} - \frac{1}{T_2}\right)\right) Ln_{T_1}\phi_{i,T_1} \quad (87)$$

Therefore:

$$\left(\frac{S_{i,j}}{S_z}\right)_{T_2} = \frac{1 + \exp\left(\left(\frac{E_{d,j}}{R}\right)\left(\frac{1}{T_1} - \frac{1}{T_2}\right)\right) Ln_{T_1}\phi_{i,T_1}}{1 + \exp\left(\frac{E_{d,i}}{R}\left(\frac{1}{T_1} - \frac{1}{T_2}\right)\right)\phi_{i,T_1}} \quad (88)$$

In the case of silicalite-1, $E_{d,water} = 13.3\ \frac{KJ}{mol}$, [45] and $E_{d,ethanol} = 10\ \frac{KJ}{mol}$, (estimate, [47])

This results in the following plot ($Ln_{T_1} = 0.0012$) of equation (88):

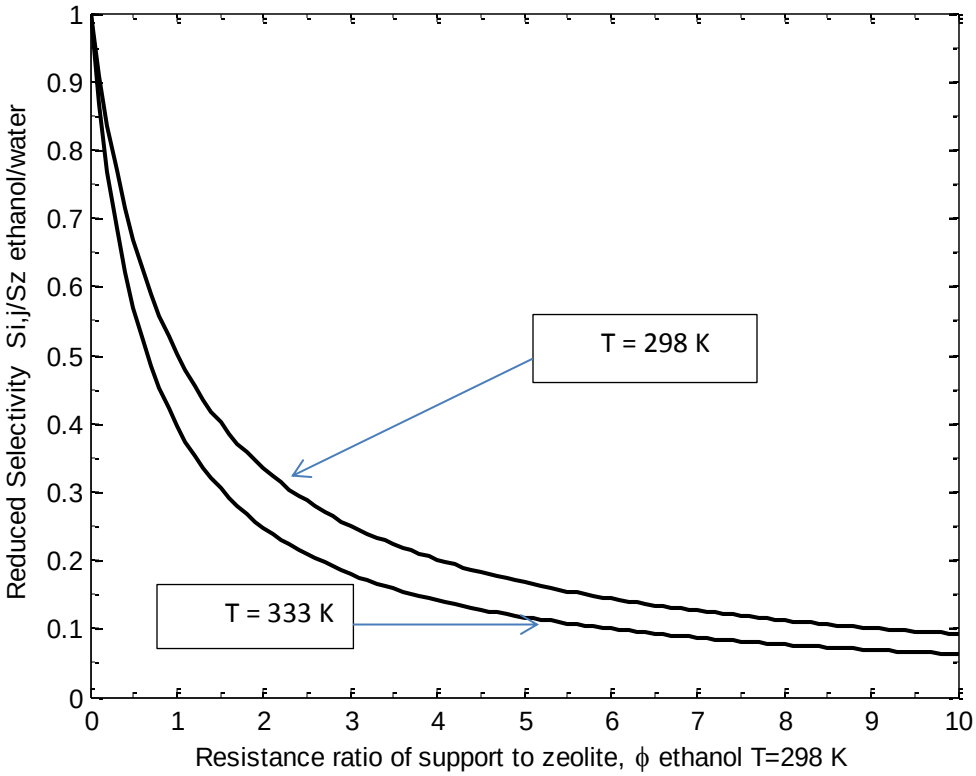

Figure 2.8

Effect of temperature on reduced selectivity with ϕ_{i,T_1} and Ln_{T_1} for ethanol at 298 K

Figure 2.8 demonstrates that the effect of relative support resistance on reduced selectivity is increased with increasing temperature. Flux is increased by increasing temperature. The increase in the ratio of ideal fluxes (i/j) is greater than the increase in the ratio of real fluxes (i/j). The effect is more significant at lower resistance ratios.

2.4 **COMPARISON OF THE CURRENT MODEL TO THE DE BRUIJN MODEL**

The de Bruijn model used a ratio of pressure drops to define mass transfer resistance in the support (eq. 16). This ratio which, for purposes of comparison, may be referred to as the resistance ratio of support to total membrane, is similar to ϕ_i and provides similar information as the flux model:

$$resistance\ to\ mass\ transfer = \frac{-\Delta p_{support,i}}{-\Delta p_{total,i}} \quad (16)$$

$$resistance\ ratio\ of\ support\ to\ zeolite, i\ (\phi_i) = \frac{-\Delta p_{support,i}}{-\Delta p_{zeolite,i}} \quad (42)$$

$$resistance\ ratio\ of\ zeolite\ to\ total\ (\Pi_i) = \frac{-\Delta p_{zeolite,i}}{-\Delta p_{total,i}} \quad (55) \quad p_{permate,i} = 0$$

Therefore:

$$resistance\ to\ mass\ transfer = (\phi_i \Pi_i) \quad (89)$$

Since equation (27) applies, the model parameters can be derived from the "$resistance\ to\ mass\ transfer$" ratio. However, equation (89) is valid only when the molar flux terms in the resistance ratios can be cancelled (as described for equation 55). Thus the de Bruijn model is solely a flux model which can only be used to describe completed pervaporation runs. It is not a selectivity model and it is not predictive as the flux and selectivity models described in this thesis are, as shown in chapter 3.

The de Bruijn study separates the results of pervaporation studies into two groups. In one group comprised mostly of dehydration separations, the flux is limited by the support. In the other group, mostly organic separations from water, the flux is not limited. The flux model, as described in this thesis, defines the reason for the flux limitation in the first group. Dehydration separations by pervaporation generally have higher zeolite layer permeances and thus higher resistance ratios of support to zeolite. The effect on real flux and relative permeation flux is described quantitatively by the flux model equation.

2.5 **CONCLUSIONS**

The resistance in series model was found to fit pervaporation in a zeolite supported membrane. In a single compnonent pervaporation, flux is identical across the membrane, and the total pressure drop is the sum of the individual pressure drops across the membrane layers. Resistance was defined as the ratio of pressure drop to flux, and is the reciprocal of permeance. The flux model introduced the dimensionless variable Π_i, relative permeation flux.

The flux model also introduced the dimensionless variable Γ_i, to include viscous flow through the support. However, it was demonstrated that up to 10-20% viscous flow had a negligible effect on Π_i as a function of ϕ_i. The flux model was then simplified to include only Knudsen flow in the support, identical to the selectivity model in that respect. As will be shown in the next chapter, the presence of a significant amount of viscous flow in the support will limit the applicability of the model equations.

The selectivity model introduced the dimensionless variable $\frac{S_{i,j}}{S_z}$, reduced selectivity. As an aid to understanding the physical meaning of the flux and selectivity models, and to facilitate comparison with the de Bruijn et al. model, both the flux and selectivity models were recast in terms of resistance ratios as ratios of pressure drops, although the recast equations can only be applied when the molar flux terms in the original equations are identical (single pervaporation run). Additionally, ϕ_i, Π_i, and $\frac{S_{i,j}}{S_z}$ were shown to be functions of temperature. ϕ_i increased with temperature. Π_i, and $\frac{S_{i,j}}{S_z}$ were shown to decrease with increasing temperature when shown as functions of ϕ_i at T_1.

The dimensionless variable ϕ_i was introduced as the resistance ratio of support to zeolite; the definition was based on 100% Knudsen flow through the support. ϕ_i is the independent variable for the flux and selectivity models. Equation (40) shows that ϕ_i can be varied by changing $F_{zeolite,i}$ or α_i. The effects of varying $F_{zeolite,i}$ and α_i will be discussed in the next chapter.

When pervaporation characterization of a feed mixture is carried out using a zeolite supported membrane, the zeolite layer permeances of the feed components can be calculated. If may then be desirable to learn what the fluxes and selectivities would be if the same zeolite layer was coupled to different supports. In that case, the only additional data needed would be the results of helium permeance studies of those additional supports. The values of the zeolite layer permeances can then be coupled with the results of the helium permeance values of those additional supports, and then the fluxes and selectivities of the to be synthesized zeolite supported membranes can be predicted using the model equations. This is the main point of this thesis, and will be further discussed in the following chapters.

CHAPTER 3

EXPERIMENTAL AND RESULTS

3.1 **OVERVIEW**

The previous chapter introduced the flux and selectivity models. The independent variable for both models is the resistance ratio of support to zeolite, species "i", ϕ_i. ϕ_i is a function of the zeolite permeance, $F_{zeolite,i}$ and the Knudsen permeance of the support, α_i.

The effect of altering the permeance of the zeolite layer can be analyzed by substituting equation (40) into equation (53) for the flux model and equation (75) for the selectivity model. Zhou et al [48]., for example, increased the permeance (eq. 44) of the zeolite layer by making the zeolite layer ultrathin. An increase in flux was observed but we can see from equation (53) that relative permeation flux will decrease since the increase in ideal flux will be greater than the increase in real flux. From equation (75), if the permeance of the zeolite layer is increased while the selectivity of the zeolite layer remains the same (the Lin number is unchanged), then reduced selectivity and real selectivity will decrease. On the other hand if the increase in permeance of the zeolite layer causes an unpredictible change in the selectivity of the zeolite layer, the effect on reduced selectivity would also be difficult to predict.

There is also current research investigating ways to increase support permeance. The general approach for increasing support permeance (decreasing support resistance) is found from examination of equation (35). It has been confirmed experimentally that increasing the porosity of the support will increase its permeance [53]. There is a limit,

depending on the support material, as to how much the porosity can be increased in terms of structural stability. Increasing support pore diameter will also increase support permeance. However, this approach is limited because too large a pore diameter will result in intrusion of the zeolite into the support during synthesis [53]. Decreasing support tortuosity in theory would lead to an increase in support permeance, but this approach does not appear to be the subject of ongoing research. Decreasing the thickness of the support will also lead to increased support. This approach has been used by Shan et al. and others to increase the flux through a zeolite supported membrane. In the Shan study, alumina hollow fibers were used to increase the flux of silicalite-1 supported membranes for pervaporation separation of ethanol from water [20].

The effect of increasing support permeance on flux can be readily evaluated by the current model through use of equations (41) and (53). Increased support permeance will result in a smaller value of the resistance ratio of support to zeolite. This will result in an increase in relative permeation flux. This effect is caused by an increase in real flux; there is no change in ideal flux through the zeolite layer.

The effect of increasing support permeance on selectivity can be evaluated by the current model through use of equations (41) and (75). In this case reduced selectivity is increased by an increase in total selectivity; the selectivity of the zeolite layer is not changed by a change in support permeance.

The objective of this chapter is to show the effect of different supports on the flux and selectivity of a silicalite-1 supported membrane, experimentally, and by using the flux and selectivity models. To accomplish this, the permeance of the original support

was decreased by adding an additional support layer, as described below. This approach is novel since support permeance is decreased rather than increased.

The next section of this chapter will describe how zeolite membranes are made and characterized in our laboratory. The strategy used to experimentally verify the flux and selectivity model will be explained. A subsequent section will present the results of the experiments done, and will also present results obtained from the literature. The ability of the flux and selectivity model equations to predict the experimental results will be analyzed. This will be followed by the conclusion.

3.2 **EXPERIMENTAL**

3.2.1 **Membrane synthesis**

Silicalite-1 suspension with a concentration of 2.0 wt% was coated onto a YSZ coated porous stainless steel support by a dip-coating method to make the silicalite seed layer. The dip-coating time was about 5 s. The coated support was dried in an oven at 40˚C with a relative humidity of 60% for 2 days, followed by calcination at 550˚C for 8 hr in air. The dip-coating and calcination of the silicalite seed layer was repeated three times to ensure complete coverage of the support with silicalite seeds. The final silicalite layer was applied by secondary growth from an alumina-free solution with composition 0.9 NaOH:0.9 TPABr:4 SiO_2:1000 H_2O:16 EtOH at 175˚C for 8 hr. The synthesized silicalite-1 supported membrane was washed and dried, then calcined at 500˚C in air to remove template [49].

3.2.2 **Experimental Method**

A pervaporation study with the as-synthesized silicalite-1 YSZ/SS supported membrane was done using an ethanol/water feed, 5 wt% ethanol, at 298 K. Following this, additional pervaporation studies were done at the same conditions by adding additional support layers, stainless steel and γ-alumina, in separate experiments. The additional support was added by physically juxtaposing it to the support side of the initial silicalite-1 YSZ/SS supported membrane in the pervaporation cell. The silicalite-1 layer was not physically or chemically altered by this process. The effect of adding the additional support layer on membrane performance could then be analyzed.

3.3.3 **Characterization**

The silicalite-1 surface morphology and cross section were examined by a Philips PEI XL-30 scanning electron microscope at accelerating voltage of 15 kV after gold deposition. Its crystal structure was examined by powder X-ray diffraction with a conventional Bruker D8 diffractometer at 20 kV, 5 mA with a scan speed of 2˚/min and a step size of 0.02˚ in 2θ, using CuKα (λ=0.1543 nm) radiation [50]. The supports were characterized by a steady state single gas (Helium) permeation system. The support was mounted in a stainless steel membrane cell and sealed by silicone O-rings. The permeation area of the support was 2.24 x $10^{-4}\ m^2$. The feed was Helium without diluent at a feed pressure of 270 kPa. The permeate side was connected to a bubble flow meter at atmospheric pressure without sweeping gas so the support permeate side was maintained at 101 kPa (1 atm). The flow rate of the feed effluent was controlled at 50 ml/min [51].

The separation performances of the initial silicalite-1 YSZ/SS supported membrane, and of the sililcalite-1 YSZ/SS supported + additional support layer membranes, were evaluated through pervaporation of 5 wt% ethanol in water at 298 K using the system described by O'Brien-Abraham et al. The permeate side of the cell was kept under vacuum at 20 Pa and the permeate was condensed into a liquid nitrogen cold trap. The mass of the condensed permeate was used to calculate the overall flux through the membrane according to J=W/(At), where W is the weight of the permeate (Kg), A is the membrane area (m^2) and t is the time (Hr) for the sample collection. The amount of ethanol in the permeate was measured with a gas chromatograph (GC, Model 8610C, SRI Instruments, Menlo Park, CA). The permeate was diluted with a known quantity of water prior to measurement by the gas chromatograph. Permeance and selectivity of the silicalite-1 YSZ/SS supported membrane, for the silicalite-1 layer and the total membrane were calculated from the measured flux and separation factor following the methodology recommended by Baker [2]. The total permeance was calculated using equation (67), permeate pressure assumed to be zero. The feed pressure for a permeating species was calculated using equation (21). The experimental results will be presented according to the following flow chart:

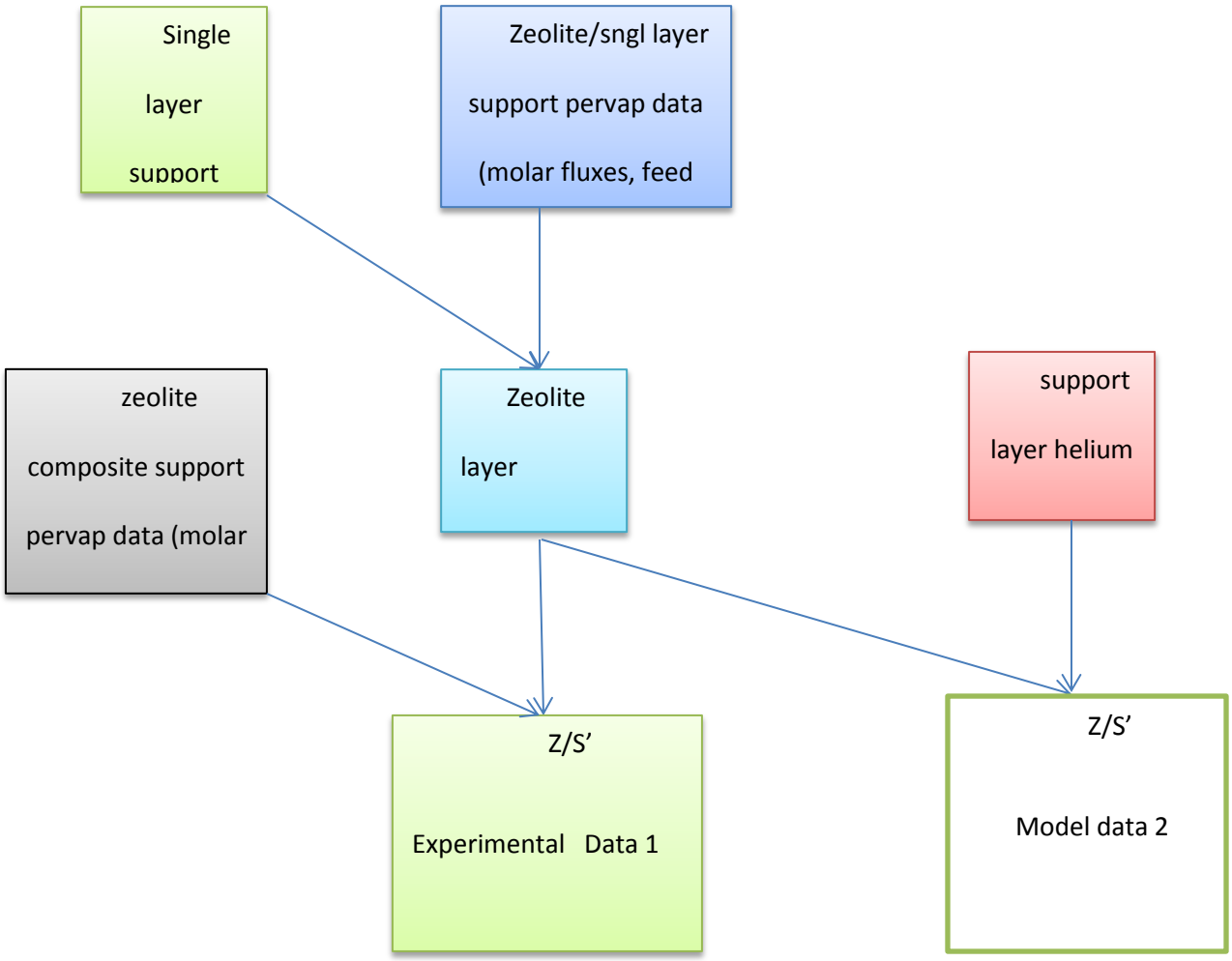

Figure 3.1

Flow chart for presentation of results

3.3 **RESULTS**

3.3.1 **Experimental Results**

Figure 3.2 shows the surface SEM image of the silicalite membrane synthesized on the YSZ modified stainless steel support. As shown, the membrane is free of any defects. In the XRD spectra of the membrane shown in Figure 3.3, the diffraction peaks from silicalte membrane layer, YSZ layer and the SS support can be clearly identified. The much stronger peaks for the siliclaite layer as compared to the peaks from support suggests a thick silicalite layer.

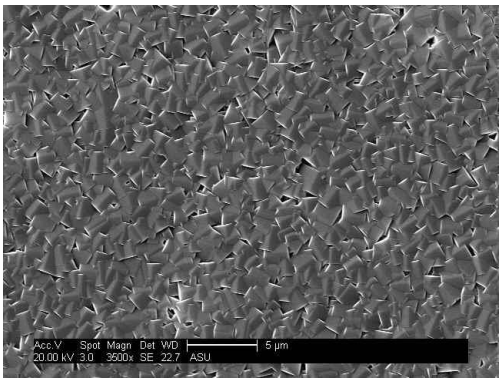

Figure 3.2

Surface SEM image of silicalite-1 membrane

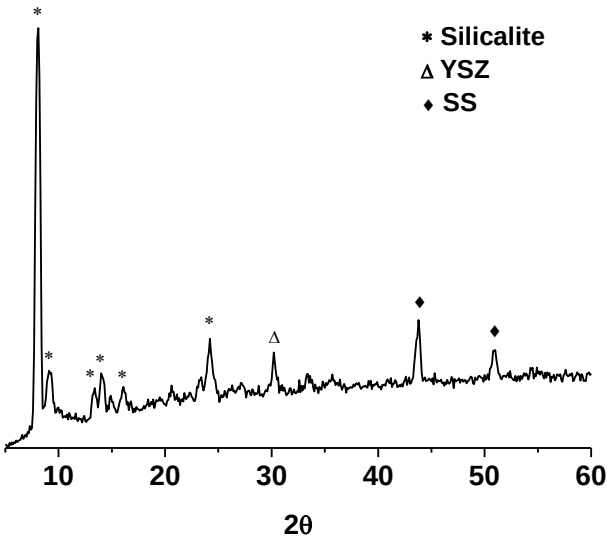

Figure 3.3

XRD of silicalite-1 membrane on YSZ/SS support

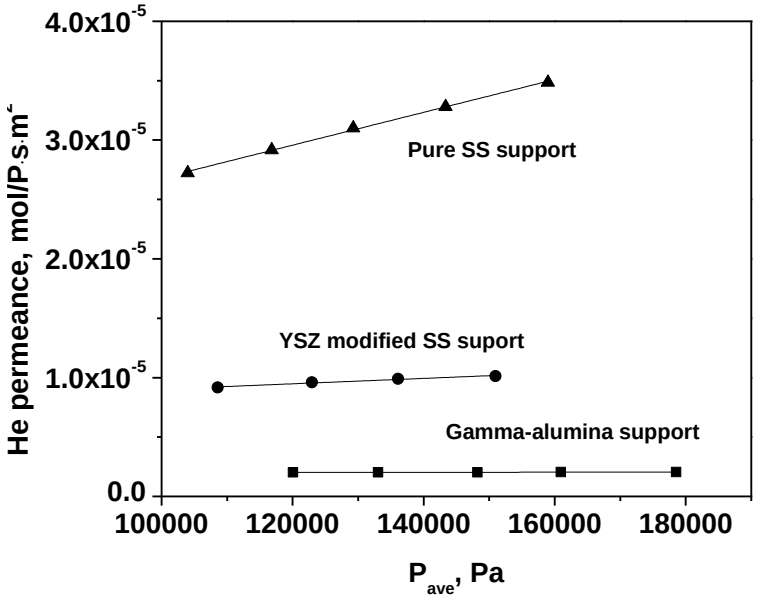

Figure 3.4

He steady state test of various supports

As per the flow chart (Figure 3.1) the first table shows the results of the Helium permeance studies for the supports. The values for α and β were converted from helium to ethanol (equations 73 and 59).

Table 3.1

Results of helium permeance

Support type	$\alpha_{ethanol}\ molsm^{-2}s^{-1}Pa^{-1}$	$\beta_{ethanol}\ molsm^{-2}s^{-1}Pa^{-2}$
YSZ/SS	1.99 x 10^{-6}	5.83 x 10^{-11}
SS	3.98 x 10^{-6}	1.18 x 10^{-12}
γ-alumina	5.81 x 10^{-7}	1.19 x 10^{-12}

Pervaporation was done using the silicalite-1 YSZ/SS supported membrane. The results of this study are presented in tables 3.2.

Table 3.2

Pervaporation characterization for silicalite-1 YSZ/SS supported membrane

Parameter	Units	Value
Feed wt% ethanol		5
Temperature	K	298
Flux	$Kgm^{-2}Hr^{-1}$	0.051
Separation Factor		21
$p_{feed,ethanol}$	Pa	753
$p_{feed,water}$	Pa	3051
$p_{interface,ethanol}$	Pa	81
$p_{interface,water}$	Pa	117
$J_{molar,ethanol}$	$molm^{-2}s^{-1}$	1.62 x 10^{-4}
$J_{molar,water}$	$molm^{-2}s^{-1}$	3.74 x 10^{-4}
$\%Knud\ flow_{ethanol}$ support		99.9
$F_{zeolite,ethanol}$	$molm^{-2}s^{-1}Pa^{-1}$	2.41 x 10^{-7}
$F_{zeolite,water}$	$molm^{-2}s^{-1}Pa^{-1}$	1.27 x 10^{-7}
S_z		1.89

Table 3.2 shows the molar fluxes computed from the flux and separation factor. The %Knudsen flow in the support was computed for ethanol using the molar flux, interfacial pressure, α, and β. $p_{interface,ethanol}$ was computed with equation (38) as was $p_{interface,water}$ (α_{water} was obtained from $\alpha_{ethanol}$ from equation (73)). The silicalite-1 permeances were computed from equation (39). The value for S_z is shown. These values are not affected by the addition of another support layer, and were used in the subsequent analysis of the two layer support pervaporation data.

Table 3.3 shows the values for total $\alpha_{ethanol}$ for the two layer supports. These values were computed using equation (31):

$$\frac{1}{\alpha_{total,ethanol}} = \frac{1}{\alpha_{\frac{YSZ}{SS},ethanol}} + \frac{1}{\alpha_{SS\ or\ \gamma-alumina,ethanol}} \quad (31)$$

Table 3.3

Values for $\alpha_{ethanol}$ for two layer supports

Support	$\alpha_{ethanol}\ molsm^{-2}s^{-1}Pa^{-1}$
YSZ/SS + SS	1.33×10^{-6}
YSZ/SS + γ-alumina	4.51×10^{-7}

Pervaporation studies were done using the silicalite-1 YSZ/SS supported membrane plus the additional support layer as described in the experimental section. The results are presented in tables 3.4 and 3.5 (the interfacial pressures were calculated using equation (38)).

Table 3.4

Pervaporation characterization silicalite-1 YSZ/SS+ stainless steel supported membrane

Parameter	Units	Value
Feed wt% EtOH		5
Temperature	K	298
Flux	$Kgm^{-2}Hr^{-1}$	0.049
Separation Factor		20.5
$p_{feed,ethanol}$	Pa	753
$p_{feed,water}$	Pa	3051
$p_{interface,ethanol}$	Pa	115
$p_{interface,water}$	Pa	171

Table 3.5

Pervaporation characterization silicalite-1 YSZ/SS+ γ-alumina supported membrane

Parameter	Units	Value
Feed wt% EtOH		5
Temperature	K	298
Flux	$Kgm^{-2}Hr^{-1}$	0.028
Separation Factor		15
$p_{feed,ethanol}$	Pa	753
$p_{feed,water}$	Pa	3051
$p_{interface,wthanol}$	Pa	165
$p_{interface,water}$	Pa	335

The following tables show the values for the model parameters. Table 3.6 shows the values for $\phi_{ethanol}$ computed by equation (40).

Table 3.6

Values for $\phi_{ethanol}$

Support	$F_{z,ethanol}\ molm^{-2}s^{-1}Pa^{-1}$	$\alpha_{ethanol}\ molm^{-2}s^{-1}Pa^{-1}$	$\phi_{ethanol}$
YSZ/SS	2.41 x 10^{-7}	1.99 x 10^{-6}	0.121
YSZ/SS + SS	2.41 x 10^{-7}	1.33 x 10^{-6}	0.181
YSZ/SS + γ-alumina	2.41 x 10^{-7}	4.51 x 10^{-7}	0.534

Table 3.7 shows the parameters for the flux model. The fourth column shows the values for $\Pi_{ethanol}$ computed from equation (50). The value of $J^0_{ethanol}$ was retained from the silicalite-1 YSZ/SS supported membrane (single support layer) pervaporation study since its value is derived from $F_{zeolite,ethanol}$ from that study. The fifth column shows the values of $\Pi_{ethanol}$ computed from equation (53). Negligible viscous flow was assumed in all cases based on the values of $\beta_{ethanol}$ for the individual support layers. The fourth column corresponds, for the two layer supports, to box 1 in the flow diagram (Figure 3.1). The fifth column, for the two layer supports, corresponds to box 2 in the flow diagram (Figure 3.1)

Table 3.7

Flux model parameters silicalite-1

Support	$J_{molar,eth}\ molm^{-2}s^{-1}$	$J^0_{molar,eth}\ molm^{-2}s^{-1}$	$\Pi_{eth}\left(\frac{J_{eth}}{J^0_{eth}}\right)$ (experimental)	Π_{eth} (eq. 53)
YSZ/SS	1.62 x 10^{-4}	1.81 x 10^{-4}	0.892	0.892
YSZ/SS+SS	1.54 x 10^{-4}	1.81 x 10^{-4}	0.851	0.850
YSZ/SS+γ-alumina	7.46 x 10^{-5}	1.81 x 10^{-4}	0.412	0.652

Table 3.8 shows the parameters for the selectivity model. $\frac{S_{i,j}}{S_z}$ was computed in two ways. For the first way, $S_{i,j}$ was computed using the molar fluxes and feed pressures according to equations (66 and 69). Then , $S_{i,j}$ was divided by the value of S_z shown in the table, and the values shown in column 4. This computation corresponds, for the two

layer supports, to box 1 in the flow diagram (Figure 3.1). $\frac{S_{i,j}}{S_z}$ was also computed using the values of Ln and $\phi_{ethanol}$, using equation (74), and the values shown in column 7. This computation corresponds, for the two layer supports, to box 2 in the flow diagram (Figure 3.1).

Table 3.8

Selectivity model parameters silicalite-1

Support	$S_{i,j}$ (eqs. 66 and 69)	S_z	$S_{i,j}/S_z$ (experimental)	$\phi_{ethanol}$	Ln	$S_{i,j}/S_z$ (eq.75)
YSZ/SS	1.75	1.89	0.926	0.121	0.331	0.926
YSZ/SS+SS	1.71	1.89	0.905	0.181	0.331	0.897
YSZ/SS+γ-alumina	1.25	1.89	0.661	0.534	0.331	0.767

An examination of tables 3.7 and 3.8 shows that, for the silicalite-1 YSZ/SS supported membrane (single layer support), the model values are identical to the experimental values. In this case, following the derivation of the model equation, equations (50) and (53) give the same value for $\Pi_{ethanol}$. For selectivity, again following the derivation of the model, equations (70) and (71) give the same value for $\frac{S_{i,j}}{S_z}$ as equation (75).

The situation clearly changes with the addition of another support layer. The stainless steel support had higher permeance (less resistance) than the YSZ/SS support.

Adding the stainless steel support to the YSZ/SS support caused an increase in support resistance, as would be expected, but the effect on the resistance ratio of the support to zeolite, $\phi_{ethanol}$, was small. Consequently, the flux and separation factor with the addition of the stainless steel support were almost the same as those obtained with the silicalite-1 YSZ/SS supported membrane (single layer support). There was < 5% difference in $\Pi_{ethanol}$ and $\frac{S_{i,j}}{S_z}$ values, as obtained from experimental data and as obtained from the model equations, for the silicalite-1 YSZ/SS+SS supported membrane and the silicalite-1 YSZ/SS supported membrane.

The γ-alumina support had lower permeance (more resistance) than the YSZ/SS support. Adding this support to the YSZ/SS support caused a larger increase in support resistance than adding the stainless steel support layer. The effect on the resistance ratio of support to zeolite was larger. Consequently the flux and separation factor were significantly less than those obtained with the silicalite-1 YSZ/SS supported membrane (single layer support). There was a much larger difference in the model values for $\Pi_{ethanol}$ and $\frac{S_{i,j}}{S_z}$ between those obtained for the silicalite-1 YSZ/SS supported membrane (single layer support) and those obtained for the silicalite-1 YSZ/SS+ γ-alumina supported membrane (two layer support). There were also significant differences between $\Pi_{ethanol}$ and $\frac{S_{i,j}}{S_z}$ obtained experimentally and $\Pi_{ethanol}$ and $\frac{S_{i,j}}{S_z}$ obtained from the model equations for the silicalite-1 YSZ/SS+ γ-alumina supported membrane (two layer support).

The significance of these findings will be discussed below. At present it is sufficient to notice that the model values for $\Pi_{ethanol}$ (column 5 in table 3.10) and $\frac{S_{i,j}}{S_z}$ (column 7 in table 3.11) for the silicalite-1 YSZ/SS+additional supports were obtained without the need for a second pervaporation study. $\phi_{ethanol}$ was obtained from the composite support data, and $F_{zeolite,ethanol}$, S_z, and Lin were retained from the original silicalite-1 YSZ/SS supported membrane (single layer support) pervaporation study. Thus the model equations give predictions of the results of the second pervaporation study.

3.3.2 **Literature examples**

The next section will review two studies from the literature. One is a case from the de Bruijn et al. study, and the second is a case from the Zhou study. The case from the de Bruijn study is a silicalite-1 supported membrane separating ethanol from water. Thus, it is the same pervaporation separation using the same zeolite as we are investigating in our laboratory. In contrast, the case from the Zhou et al. study is a zeolite-X supported membrane used for the pervaporation dehydration of ethanol. The method of data presentation will follow that used for the presentation of experimental results (Figure 3.1), although no additional support layers were added in these studies. It is important to note that species "i" for the de Bruijn study is ethanol; for the Zhou study it is water. The support in the de Bruijn study [23] was an α-alumina disc; the support in the Zhou study [48] was a two layer alumina disc. The data for the supports is shown in table 3.9.

Table 3.9

Support values, literature

Support	$\alpha_i\ molsm^{-2}s^{-1}Pa^{-1}$	$\beta_i\ molsm^{-2}s^{-1}Pa^{-2}$	%Knudsen
α-alumina [21]	1.51 x 10^{-5}	8.74 x 10^{-10}	98
Alumina int layer [46]	1.46 x 10^{-5}	2.04 x 10^{-10}	94
Alumina bot layer	1.02 x 10^{-5}	9.12 x 10^{-9}	35
Int+bottom	6.00 x 10^{-6}	-	-

The value for α_i for "Int+bottom" in table 3.9 is a composite value calculated from the values of α_i from the individual layers using equation (30), assuming 100% Knudsen flow. The values for %Knudsen flow in table 3.9 and the values for the interfacial pressures in table 3.10 were obtained using equations (11-14). Since the total flux is known, and the values for the constants were given, equations (11, 13, and 15) provide a solution for the interfacial pressure. Table 3.10 shows the results of the pervaporation studies.

Table 3.10

Pervaporation characterization, literature

Parameter	Units	De Bruijn	Zhou
zeolite		Silicalite-1	X
support		α-alumina	Two layer alumina
Species "i"		ethanol	water
Feed wt% EtOH		5	90
Temperature	K	333	338
Flux	$Kgm^{-2}Hr^{-1}$	1.8	3.37
Separation factor		89	296
$p_{feed,water}$	Pa	19224	10982
$p_{feed,ethanol}$	Pa	4495	46813
$p_{interface,water}$	Pa	202	6180
$p_{interface,ethanol}$	Pa	593	166

Next the values for ϕ_i were calculated using equation (40). The zeolite permeances were obtained by using equation (39).

Table 3.11

Values for ϕ_i, literature

Study	$F_{z,i}\ molm^{-2}s^{-1}Pa^{-1}$	$\alpha_i\ molm^{-2}s^{-1}Pa^{-1}$	ϕ_i
De Bruijn	2.30 x 10^{-6}	1.51 x 10^{-5}	0.152
Zhou	1.05 x 10^{-5}	6.00 x 10^{-6}	1.75

Finally, the model parameters were computed following the methodology as explained for tables 3.7 and 3.8.

Table 3.12

Flux model values, literature

Study	$J^0_{molar,i}\ molm^{-2}s^{-1}$	$J^0_{molar,i}\ molm^{-2}s^{-1}$	$\Pi_i\left(\frac{J_i}{J_i^0}\right)$ (experimental)	Π_i (eq. 53)
De Bruijn	0.00895	0.0103	0.870	0.868
Zhou	0.0505	0.103	0.490	0.363

Table 3.13

Selectivity model values, literature

Study	$S_{i,j}$ (eqs. 66 and 69)	S_z	$S_{i,j}/S_z$ (experimental)	ϕ_i	Ln	$S_{i,j}/S_z$ (eq.75)
De Bruijn	7.84	8.94	0.877	0.152	0.0700	0.877
Zhou	402	827	0.486	1.75	0.00193	0.365

The use of the model to analyze the silicalite-1 α-alumina supported membrane [23] for pervaporation separation of ethanol from water appears to be reliable. The experimental values for Π_i and $S_{i,j}/S_z$ were virtually identical to their model counterparts, as they were for the silicalite-1 YSZ/SS supported membrane. There was a < 1% difference in the Π_i values possibly due to a small amount of viscous flow in the support. There were difficulties in using the model to analyze the data from the Zhou study. The problems were:

1. The permeate pressure was not zero. Therefore, one of the underlying assumptions of the model was not satisfied.
2. A two layer support with each layer being significantly different in pore size and thickness was used.
3. There was a large amount of viscous flow in the support particularly in the bottom layer.

Because of these problems, the model would have to be used with caution for a membrane system such as used in the Zhou study.

3.4 **CONCLUSIONS**

When the flux and selectivity models were applied to the silicalite-1 YSZ/SS supported membrane from our laboratory, and to the silicalite-1 α-alumina supported membrane from the de Bruijn study, the model values were the same as the experimental values. In both cases, the underlying assumptions of the model, negligible viscous flow in the support and zero permeate pressure were met. In both cases, equation (56) can be

used to compute Π_i and equation (79) can be used to compute $S_{i,j}/S_z$, using the pressure terms supplied, and give identical results as equations (53) and (75).

As mentioned, the flux and selectivity models offer the ability to predict the results of the resultant pervaporation obtained by adding the additional support layer from the composite support data and the original permeances from the original (silicalite-1 YSZ/SS supported membrane) pervaporation run. In the case of the added stainless steel support, the effect on $\phi_{ethanol}$ was small, and the model was in good agreement with the experimental values. In the case of the added γ-alumina support there was a larger effect on $\phi_{ethanol}$. The model then overestimated the experimental relative permeation flux (37%) and reduced selectivity (14%). In terms of the raw data, a separation factor of 16.5 and a total flux of 0.041 $Kgm^{-2}Hr^{-1}$would have brought the experimental relative permeation flux and reduced selectivity to within 5% of the model values.

CHAPTER 4

SUMMARY AND RECOMMENDATIONS

4.1 **SUMMARY**

Chapter 1 provided an overview of pervaporation, a membrane separation process. A description of zeolites and zeolite membranes used in pervaporation was given. The use of the silicalite-1, a zeolite membrane, in pervaporation was reviewed, as was its specific use for ethanol/water separation. As delineated in chapter 1, if the flux and selectivity of this separation can be improved, then it will be of use industrially for the manufacture of ethanol with a bioreactor. Mathematical models of pervaporation were described as a means to evaluate and improve zeolite supported membrane performance. The limitations of previous models were discussed.

Chapter 2 introduced new models for flux and selectivity for zeolite supported membranes in pervaporation. The model equations incorporate the dimensionless variables, resistance ratio of support to zeolite, relative permeation flux, reduced selectivity and Lin number. The resistance ratio of support to zeolite is the independent variable for the flux and selectivity model equations. It is formed by the ratio of zeolite to support permeances. The model equations were also formulated as ratios of pressure drops across the membrane layers. This allowed for comparison to the de Bruijn model. By this comparison the de Bruijn model was shown to be a descriptive model of flux, whereas the new model also includes selectivity and is predictive. Equations showing the temperature dependence of the flux and selectivity model equations were introduced.

Chapter 3 described experiments designed to show how the model equations could predict the effects of different supports on flux and selectivity. In a novel

approach, support resistance was increased by adding an additional support layer. When a stainless steel support was added, the model equations predicted results that were close to those obtained experimentally. The agreement was not as close when an additional γ-alumina support was added. It is difficult to assess the significance of these findings since the data is limited. The model equations were also used to analyze two examples from the literature. The application of them model equations to one of these examples from the Zhou study was limited because of significant viscous flow in the bottom support layer.

An overall summary of the utility of the model may now be provided. The flux model relates two dimensionless parameters, relative permeation flux and the resistance ratio of the support to zeolite. Relative permeation flux is the ratio of real flux to the ideal flux of the stand- alone zeolite layer and has a maximum value of one. As mentioned in chapter 1, the flux through a support is in general significantly higher than the ideal flux of a stand-alone zeolite layer. The effect, due to resistance in series, of adding a support layer to the zeolite layer is to diminish real flux and relative permeation flux. The effect on real flux and relative permeation flux is determined by the resistance ratio of the support to zeolite. As support resistance increases (permeance decreases), real flux and relative permeation flux decrease in a way that is described by the flux model. When a zeolite layer is synthesized onto a support, real flux and ideal flux are determined by pervaporation of a feed mixture. The model assumes that a similar zeolite layer can be synthesized onto other supports so that ideal flux remains the same. The model then predicts the effect of the supports on real flux based on the results of helium permeance studies of the supports. From a practical standpoint, there would be no need

to actually carry out the synthesis on the other supports and perform pervaporation studies because the results of those pervaporation studies can be predicted by the model in advance.

A similar conclusion can be reached with regard to selectivity. The selectivity model relates three dimensionless parameters, reduced selectivity, Lin number, and the resistance ratio of the support to zeolite. The model assumes that the Lin number, the ratio of support selectivity to zeolite selectivity will be less than one. Reduced selectivity, the ratio of real selectivity to the selectivity of the zeolite layer has a maximum value of one. When a zeolite layer is synthesized onto a support, real selectivity and the selectivity of the zeolite layer are determined by pervaporation of a feed mixture. The model assumes that a similar zeolite layer can be synthesized onto other supports so that the selectivity of the zeolite layer remains the same. Assuming Knudsen flow in the supports, the selectivity of the supports also remains the same since support selectivity is determined by the square root of the ratio of molecular weights of the feed components. Therefore the Lin number remains the same. The model then predicts the effect of the supports on real selectivity based on the results of helium permeance studies of the supports. From a practical standpoint there would be no need to actually carry out the synthesis of the zeolite layer onto the other supports and perform pervaporation studies because the results of those pervaporation studies can be predicted by the model in advance.

On the other hand, it may be argued that a simple intuitive grasp of the resistance in series concept leads to the same conclusions. It can be predicted that supports with higher permeances will, when synthesized into a zeolite supported

membrane, provide higher pervaporation fluxes then supports with lower permeances. However this is a qualitative prediction while the prediction offered by the flux model is quantitative. The selectivity model shows that supports with higher permeances will result in zeolite supported membranes with higher selectivity. It would be more difficult to reach the same conclusion based on an intuitive grasp of the resistance in series concept.

In brief: Once the zeolite layer permeances of the components of a given feed mixture are determined through pervaporation testing of a zeolite supported membrane, and assuming that those zeolite permeances remain the same when the zeolite layer is applied to other supports to create additional zeolite supported membranes, the flux and selectivity of the additional zeolite supported membranes as would be determined by pervaporation testing are predicted in advance of the synthesis of the additional zeolite supported membranes by the model equations.

4.2 **RECOMMENDATIONS**

1. Conduct additional experiments using the same methodology described in chapter 3. More data will provide information about the predictive power of the model equations.
2. Design and conduct experiments to evaluate the ability of the model to predict temperature dependency.

REFERENCES

[1] J. Obrien-Abraham, Y.S. Lin, Effect of Isomorphous Metal Substitution in Zeolite Framework on Pervaporation Xylene-Separation of MFI-Type Zeolite Membranes, **Ind. Eng. Chem. Res.** 49 (2010) 809-816

[2] R.W. Baker, Membrane Technology and Applications 3rd edition, John Wiley & Sons, Ltd., New York, 2012

[3] X. Feng, R.Y.M. Huang, Liquid Separation by Membrane Pervaporation: A Review, **Ind. Eng. Chem. Res.** 36 (1997) 1048-1066

[4] S. Wee, C. Tye, S. Bhatia, Membrane separation process-Pervaporation through zeolite membrane, **Sep. Purif. Technol**. 63 (2008) 500-516

[5] D.A. Fedosov, A.V. Smirnov, E.E. Knyazeva, I.I. Ivanova, Zeolite Membranes: Synthesis, Properties, and Applications, **Petroleum Chemistry** 51 (2011) 657-667

[6] J. Caro, M. Noack, P. Kolsch, R. Schafer, Zeolite Membranes-state of their development and perspective, **Microporous and Mesoporous Materials** 38 (2000) 3-24

[7] J. Caro, M. Noack, Zeolite Membranes-Recent developments and progress, **Microporous and Mesoporous Materials** 115 (2008) 215-233

[8] L.M. Vane, A review of pervaporation for product recovery from biomass fermentation processes, **Journal of Chemical Technology and Biotechnology** 80 (2005) 603-629

[9] C. Dawson, Zeolites: Structural Properties and Benchmarks of Feasibility, PhD. Thesis, ASU dept. of physics (2013)

[10] Y.S. Lin, I. Kumakiri, B.N. Nair, H. Alsyouri, Microporous Inorganic Membranes, **Separation and Purification Methods** 31 (2002) 229-379

[11] E. M. Flanigen, J. M. Bennett, R. W. Grose, J. P. Cohen, R. L. Patton, R. M. Kirchner & J. V. Smith, Silicalite, a new hydrophobic crystalline silica molecular sieve, **Nature** 271 (1978) 512-516

[12] D.M. Bibby, N.B. Milestone, L.P. Aldridge, Silicalite-2, a silica analogue of the aluminosilicate zeolite ZSM-11, **Nature** 280 (1979) 664-665

[13] A.F. Masters, T. Maschmeyer, Zeolites-From curiosity to cornerstone, **Microporous and Mesoporous Materials** 142 (2011) 423-438

[14] M.P. Pina, R. Mallada, M. Arruebo, M. Uriztondo, N. Navascues, O. de la Iglesia, J. Santamaria, Zeolite films and membranes. Emerging applications, **Microporous and Mesoporous Materials** 114 (2011) 19-27

[15] T. Bowen, R. Noble, J. Falconer, Fundamentals and applications of pervaporation through zeolite membranes, **Journal of Membrane Science** 245 (2004) 1-33

[16] H. Negishi, R. Mizuno, H. Yanagishita, D. Kitamoto, T. Ikegami, H. Matsuda, Preparation of the silicalite membranes using a seeding technique under various hydrothermal conditions, **Desalination** 144 (2002) 47-52

[17] M. Nomura, T. Yamaguchi, S. Nakao, Ethanol/water transport through silicalite membranes, **J. Membr. Sci.** 144 (1998) 161-171

[18] T. Sano, H. Yanagishita, Y. Kiyozumi, F. Mizukami, K. Haraya, Separation of ethanol/water mixture by silicalite membrane on pervaporation, **J. Membr. Sci.** 95 (1994) 221-228

[19] X. Lin, H. Kita, K. Okamoto, Silicalite Membrane Preparation, Characterization and Separation Performance, **Ind. Eng. Chem. Res.** 40 (2001) 4069-4078

[20] L. Shan, J. Shau, Z. Wang, Y. Yan, Preparation of zeolite MFI membranes on alumina hollow fibers with high flux for pervaporation, **J. Membr. Sci.** 378 (2011) 319-329

[21] X. Shu, X. Wang, Q. Kong, X. Gu, N. Xu, High-Flux MFI Zeolite Membrane Supported on YSZ Hollow Fiber for Separation of Ethanol/Water, **Ind. Eng. Chem. Res.** 51 (2012) 12073-12080

[22] D. Korelskiy, T. Lappajarvi, H. Zhou, M. Grahn, J. Tanskanen, H. Hedlund, High flux MFI membranes for pervaporation, **J. Membr. Sci.** 427 (2013) 381-389

[23] F.T. de Bruijn, L. Sun, Z. Olujic, P.J. Jansens, F. Kapteijn, Influence of the support layer on the flux limitation in pervaporation, **J. Membr. Sci.** 223 (2003) 141-156

[24] E.E. McLeary, J.C. Jansen, F. Kapteijn, Zeolite based films, membranes and membrane reactors: Progress and prospects, , **Microporous and Mesoporous Materials** 90 (2006) 198-220

[25] B. Bettens, A. Verhoef, H. van Veen, C. Vancecasteele, Pervaporation of binary water-alcohol and methanol-alcohol mixtures through microporous methylated silica membranes: Maxwell-Stefan modeling, **Computers and Chemical Engineering** 34 (2010) 1775-1778

[26] M. Yu, Separation Mechanisms and Microstructure Characterization of Zeolite Membranes, PhD. Thesis, University of Colorado Department of Chemical and Biological Engineering (2007)

[27] D.M. Ruthven, Fundamentals of Adsorption Equilibrium and Kinetics in Microporous Solids, **Mol. Sieves** 7 (2008) 1-43

[28] J. Kuhn, R. Stemmer, F. Kaptejin, S. Kjelstrup, J. Gross, A non-equilibrium thermodynamics approach to model mass and heat transport for water pervaporation through a zeolite membrane, **J. Membr. Sci.** 330 (2009) 388-398

[29] R.B. Bird, W.E. Stewart, E.N. Lightfoot, Transport Phenomena, 2nd edition, John Wiley & Sons, Inc. New York (2007)

[30] V.A. Tuan, S. Li, J.L. Falconer, R.D. Noble, Separating organics from water by pervaporation with isomorphously-substituted MFI zeolite membranes, **J. Membr. Sci.** 196 (2002) 111–123

[31] R.W. van Gemert, F.P. Cuperus, Newly developed ceramic membranes for dehydration and separation of organic mixtures by pervaporation, **J. Membr. Sci**. 105 (1995) 287–291

[32] W. Chen, C.R. Martin, Highly methanol-selective membranes for the pervaporation separation of methyl t-butyl ether/methanol mixtures, **J. Membr. Sci.** 104 (1995) 101–108

[33] B.N. Nair, K. Keizer, H. Suematsu, Y. Suma, N. Kaneko, S. Ono, T. Okubo, S.-I. Nakao, Synthesis of gas and vapor molecular sieving silica membranes and analysis of pore size and connectivity, **Langmuir** 16 (2000) 4558–4562

[34] M. Asaeda, J. Yang, Y. Sakou, Porous silica-zirconia (50%) membranes for pervaporation of iso-propyl alcohol (IPA)/water mixtures, **J. Chem. Eng. Japan** 35 (4) (2002) 365–371

[35] T. Sano, M. Hasegawa, Y. Kawakami, H. Yanagishita, Separation of methanol/methyl-tert-butyl ether mixture by pervaporation using silicalite membrane, **J. Membr. Sci**. 107 (1995) 192–196

[36] C.J. Gump, X. Lin, J.L. Falconer, R.D. Noble, Experimental configuration and adsorption effects on the permeation of C4 isomers through ZSM-5 zeolite membranes, **J. Membr. Sci**. 173 (2000) 35–52

[37] M.K. Koukou, N. Papayannakos, N.C. Markatos, M. Bracht, H.M. Van Veen, A. Roskam, Performance of ceramic membranes at elevated pressure and temperature: effect of non-ideal flow conditions in a pilot scale membrane separator, **J. Membr. Sci**. 155 (1999) 241–259

[38] H.M. van Veen, Y.C. van Delft, C.W.R. Engelen, P.P.A.C. Pex, Dewatering of organics by pervaporation with silica membranes, **Gas Sep. Purif. Technol**. 22–23 (2001) 361–366

[39] C.M. Braunbarth, L.C. Boudreau, M. Tsapatsis, Synthesis of ETS-4/TiO2 composite membranes and their pervaporation performance, **J. Membr. Sci**. 174 (2000) 31–42

[40] Y. Morigami, M. Kondo, J. Abe, H. Kita, K. Okamoto, The first large-scale pervaporation plant using tubular-type module with zeolite NaA membrane, **Sep. Purif. Technol**. 25 (2001) 251–260

[41] M. Kondo, M. Komori, H. Kita, K. Okamoto, Tubular-type pervaporation module with zeolite NaA membrane, **J. Membr. Sci**. 133 (1997) 133–141

[42] K. Okamoto, H. Kita, K. Horii, K. Tanaka, Zeolite NaA membrane: preparation, single-gas permeation, and pervaporation and vapor permeation of water/organic liquid mixtures, **Ind. Eng. Chem. Res**. 40 (2001) 163–175

[43] A.W. Verkerk, P. van Male, M.A.G. Vorstman, J.T.F. Keurentjes, Description of dehydration performance of amorphous silica pervaporation membranes, **J. Membr. Sci**. 193 (2001) 227–238

[44] M. Asaeda, J. Yang, Y. Sakou, Porous silica-zirconia (50%) membranes for pervaporation of iso-propyl alcohol (IPA)/water mixtures, **J. Chem. Eng. Japan** 35 (4) (2002) 365–371

[45] P. Kölsch, M. Sziládi, M. Noack, J. Caro, L. Kotsis, I. Kotsis, I. Sieber, Ceramic membranes for water separation from organic solvents, **Chem. Eng. Technol**. 25 (2002) 357–362

[46] S. Li, V.A. Tuan, R.D. Noble, J.L. Falconer, Pervaporation of water/THF mixtures using zeolite membranes, **Ind. Eng. Chem. Res**. 40 (2001) 4577–4585

[47] J.Z. Yang, Y. Chen, A.M. Zhu, Q.L. Liu, J.Y. Wu, Analyzing diffusion behaviors of methanol/water through MFI membranes by molecular simulation, **J. Membr. Sci** 318 (2008) 327-333

[48] H. Zhou, D. Korelskiy, T. Leppajarvi, M. Grahn, J. Tanskanen, J. Hedlund, Ultrathin zeolite X membranes for pervaporation dehydration of ethanol, **J. Membr. Sci** 399-400 (2012) 106-111

[49] H. Wang, Y.S. Lin, Synthesis and modification of ZSM-5/silicalite bilayer membrane with improved hydrogen separation performance, **J. Membr. Sci**. 396 (2012) 128-137

[50] D. Liu, X. Ma, H. Xi, Y.S. Lin, Gas transport properties and propylene/propane separation characteristics of ZIF-8 membranes, **J. Membr. Sci**. 451 (2014) 85-93

[51] Z. Zhau, X. Ma, Z. Li, Y.S. Lin, Synthesis, characterization and gas transport properties of MOF-5 membranes, **J. Membr. Sci**. 382 (2011) 82-90

[52] A. Yadav, M.L. Lind, X. Ma, Y.S. Lin, Nanocomposite Silicalite-1/Polydimethylsiloxane Membranes for Pervaporation of Ethanol from Dilute Aqueous Solutions, **Ind. Eng. Chem. Res**. 52 (2013) 5207-5212

[53] Z.B. Wang, Q.Q. Ge, J. Shau, Y.S. Yan, High performance zeolite LTA pervaporation membranes on ceramic hollow fibers by dipcoating-wiping seed deposition, **J. Am. Chem. Soc.** 131 (2009) 6910-6911

APPENDIX A

THE FLUX MODEL

The first portion of the model is for flux, assuming single species permeation through the membrane.

First, considering the zeolite layer:

$$-F_{zeolite,i}\Delta p_{zeolite,i} = F_{zeolite,i}\left(p_{feed,i} - p_{interface,i}\right) \quad (1)$$

And then the support layer:

$$F_{support,i}\Delta p_{support,i} = (\alpha_i + \beta p_{ave,i})\Delta p_{support,i} \quad (2)$$

Equation (2) can be rearranged:

$$-(\alpha_i + \beta p_{ave,i})\Delta p_{support,i} = \alpha_i\left(p_{interface,i} - p_{permeate,i}\right) + \frac{\beta}{2}((p_{interface,i})^2 - \left(p_{permeate,i}\right)^2) \quad (3)$$

Equations (1) and (3) are equations for flux through the zeolite layer and support, respectively. Since these fluxes are equal:

$$F_{zeolite,i}\left(p_{feed,i} - p_{interface,i}\right) = \alpha_i\left(p_{interface,i} - p_{permete,i}\right) + \frac{\beta}{2}((p_{interface,i})^2 - \left(p_{permeate,i}\right)^2) \quad (4)$$

Equation (4) is then solved for $p_{interface,i}$ (positive root):

$$p_{interface,i} = -\left(\alpha_i + F_{zeolite,i}\right)/\beta + \{(\alpha_i + F_{zeolite,i})^2 + 2\beta[\frac{\beta}{2}(p_{permeate,i})^2 + \alpha_i p_{permeate,i} + F_{zeolite,i}x_i\gamma_i p_i^{sat}]\}^{1/2}/\beta \quad (5)$$

This first expression (equation 5) for $p_{interface,i}$ differs from that obtained by solving

$$\alpha_i + \beta \frac{p_{interface,i} + p_{permeate,i}}{2} = \frac{molar\ flux, i}{\left(p_{interface,i} - p_{permeate,i}\right)} \quad (6)$$

for $p_{interface,i}$. Both expressions are useful.)

Then substitute this first expression (eq. 5) for $p_{interface,i}$ into the equation (1) and utilize:

$$molar\ flux, i, total = molar\ flux, i, zeolite \quad (7)$$

This leads to:

$J_{molar,i} = F_{zeolite,i} x_i \gamma_i p_i^{sat} - F_{zeolite,i}$(-$(\alpha_i + F_{zeolite,i}) + \{(\alpha_i + F_{zeolite,i})^2 +$

$2\beta[\frac{\beta}{2}(p_{permeate,i})^2 + \alpha_i p_{permeate,i} + F_{zeolite,i} x_i \gamma_i p_i^{sat}]\}^{1/2})/\ \beta$ (8)

$J_i^o =$

$F_{zeolite,i}(x_i \gamma_i p_i^{sat} - p_{permeate,i})$ $ideal\ flux\ through\ zeolite\ layer, no\ support$ (9)

Dividing equation (8) by equation (9) results in:

$\frac{J_{molar,i}}{J_i^o} =$ [$\beta x_i \gamma_i p_i^{sat}$- (-

$(\alpha_i + F_{zeolite,i}) + \{(\alpha_i + F_{zeolite,i})^2 + 2\beta[\frac{\beta}{2}(p_{permeate,i})^2 +$

$\alpha_i p_{permeate,i} + F_{zeolite,i} x_i \gamma_i p_i^{sat}]\}^{1/2})$ /$\beta(x_i \gamma_i p_i^{sat} - p_{permeate,i})$ (10)

Or; $\frac{J_{molar,i}}{J_i^o} = \left[\frac{x_i \gamma_i p_i^{sat}}{x_i \gamma_i p_i^{sat} - p_{permeate,i}}\right] -$ (-$(\alpha_i + F_{zeolite,i}) + \{(\alpha_i + F_{zeolite,i})^2 +$

$2\beta[\frac{\beta}{2}(p_{permeate,i})^2 + \alpha_i p_{permeate,i} + F_{zeolite,i} x_i \gamma_i p_i^{sat}]\}^{1/2})$ /$\beta(x_i \gamma_i p_i^{sat} - p_{permeate,i})$

(11)

A simplifying assumption is to let the permeate pressure, $p_{permeate,i}$, equal zero. This assumption is based on the use of a vacuum on the permeate side.

When $p_{permeate,i} = 0$;

$$J_{molar,i} = F_{zeolite,i} x_i \gamma_i p_i^{sat} - \frac{F_{zeolite,i}}{\beta} \{-(\alpha_i + F_{zeolite,i}) + [(\alpha_i + F_{zeolite,i})^2 +$$

$$2\beta F_{zeolite,i} x_i \gamma_i p_i^{sat}]^{\frac{1}{2}}\} \quad (12)$$

$$J_i^o = F_{zeolite,i} x_i \gamma_i p_i^{sat} \quad (13)$$

$$\frac{J_{molar,i}}{J_i^o} =$$

$$1 - \frac{1}{\beta x_i \gamma_i p_i^{sat}} \{-(\alpha_i + F_{zeolite,i}) + [(\alpha_i + F_{zeolite,i})^2 + 2\beta F_{z,i} x_i \gamma_i p_i^{sat}]^{\frac{1}{2}}\} \quad (14)$$

Definitions:

$$\Pi_i = \frac{J_{molar,i}}{J_i^o}, the\ ratio\ of\ real\ flux\ to\ ideal\ flux \quad (15)$$

$$\phi_i = \frac{F_{zeolite,i}}{\alpha_i} \qquad \frac{resistance, support, i\ (Knudsen)}{resistance, zeolite, i} \quad (16)$$

$$\Gamma_i = \frac{\beta x_i \gamma_i p_i^{sat}}{\alpha_i} \qquad relative\ importance\ of\ the\ support\ pore\ size, i \quad (17)$$

It may also be observed:

$$\Gamma_i \frac{p_{ave,i}}{x_i \gamma_i p_i^{sat}} = \frac{-\beta p_{ave,i} \Delta p_{support,i}}{-\alpha_i \Delta p_{support,i}} \quad (18)$$

$$\frac{-\beta p_{ave,i} \Delta p_{support,i}}{-\alpha_i \Delta p_{support,i}} = \frac{J_{vis,i}}{J_{Kn,i}} \quad (19)$$

$$\Gamma_i = \frac{J_{vis,i}}{J_{Kn,i}} \frac{x_i \gamma_i p_i^{sat}}{p_{ave,i}} \quad (20)$$

Substituting these definitions into

$$\frac{J_{molar,i}}{J_i^o} = 1 - \frac{1}{\beta x_i \gamma_i p_i^{sat}} \{-(\alpha_i + F_{zeolite,i}) + [(\alpha_i + F_{zeolite,i})^2 + 2\beta F_{zeolite,i} x_i \gamma_i p_i^{sat}]^{\frac{1}{2}}\}$$

(14)

gives the equation for the flux model:

$$\Pi_i = 1 - \frac{1}{\Gamma_i}\{[(1+\phi_i)^2 + 2\phi_i\Gamma_i]^{\frac{1}{2}} - (1+\phi_i)\} \quad (21)$$

Influence of temperature on flux:

$$\Pi_i = 1 - \frac{1}{\Gamma_i}\{[(1+\phi_i)^2 + 2\phi_i\Gamma_i]^{\frac{1}{2}} - (1+\phi_i) \quad (21)$$

$$\phi_i = \frac{F_{zeolite,i}}{\alpha_i} \quad (16)$$

$$\Gamma_i = \frac{\beta x_i \gamma_i p_i^{sat}}{\alpha_i} \quad (17)$$

From the section on temperature dependence of ϕ_i (Chapter 2):

$$\phi_{i,T_2} = \exp\left(\frac{E_{d,i}}{R}\left(\frac{1}{T_1} - \frac{1}{T_2}\right)\right)\phi_{i,T_1} \quad (22)$$

Analysis of the temperature dependence of Γ_i:

The temperature dependence of β:

$$\beta = 0.125\frac{1}{L}\frac{\varepsilon}{\tau}\frac{r^2}{\mu RT} \quad (23)$$

It will be assumed that viscosity is constant over the range of temperatures considered. This is necessary because there is no readily obtainable formula for the temperature dependence of viscosity at the relevant temperatures and pressures. The viscosity is obtained by analysis of empirical plots [27].

Therefore:

$$\beta_{T_2} = \frac{T_1}{T_2}\beta_{T_1} \quad (24)$$

The temperature dependence of $x_i\gamma_i p_i^{sat}$:

The mole fraction and activity coefficient (as determined by the Van Laar equation) are not temperature dependent. From the Antoine equation the temperature dependence of p_i^{sat} is:

$$p_{i,T_2}^{sat} = \exp\left(\left(\frac{B}{T_1 + C}\right) - \left(\frac{B}{T_2 + C}\right)\right) p_{i,T_1}^{sat} \quad (25)$$

The temperature dependence of α_i from the section on the temperature dependence of selectivity:

$$\alpha_{i,T_2} = \sqrt{\frac{T_1}{T_2}}\,\alpha_{i,T_1} \quad (26)$$

Therefore:

$$\Gamma_{i,T_2} = \sqrt{\frac{T_1}{T_2}} \exp\left(\left(\frac{B}{T_1 + C}\right) - \left(\frac{B}{T_2 + C}\right)\right) \Gamma_{i,T_1} \quad (27)$$

And:

$$\Pi_{i,T_2} = 1 - \frac{1}{\sqrt{\frac{T_1}{T_2}} \exp\left(\left(\frac{B}{T_1 + C}\right) - \left(\frac{B}{T_2 + C}\right)\right)\Gamma_{i,T_1}} \{[(1 + \exp\left(\frac{E_{d,i}}{R}\left(\frac{1}{T_1} - \frac{1}{T_2}\right)\right)\phi_{i,T_1}$$

$$)^2 + 2\sqrt{\frac{T_1}{T_2}} \exp\left(\left(\frac{B}{T_1 + C}\right) - \left(\frac{B}{T_2 + C}\right)\right)\Gamma_{i,T_1} \exp\left(\frac{E_{d,i}}{R}\left(\frac{1}{T_1} - \frac{1}{T_2}\right)\right)\phi_{i,T_1}$$

$$]^{\frac{1}{2}} - \left(1 + \exp\left(\frac{E_{d,i}}{R}\left(\frac{1}{T_1} - \frac{1}{T_2}\right)\right)\phi_{i,T_1}\right)]\} \quad (28)$$

APPENDIX B

THE SELECTIVITY MODEL

The selectivity model assumes 100% Knudsen flow (i.e. $\beta = 0$) through the support, in addition to $p_{permeate,i} = 0$. The derivation of this portion of the model is as follows:

First write the equations for flux through the zeolite layer and flux through the support:

$$J_{molar,i} = F_{zeolite,i}\left(p_{feed,i} - p_{interface,i}\right) \quad (1)$$

$$J_{molar,i} = \alpha_i p_{interface,i} \quad (2)$$

$$\alpha_i = Knudsen\ permeance, support, species\ i$$

$$F_{zeolite,i} = permeance\ of\ zeolite\ layer, species\ \text{i}$$

$$p_{interface,i} = pressure\ at \frac{zeolite}{support}\ interface, species\ \text{i}$$

Equate the equations for $J_{molar,i}$ and solve for $p_{interface,i}$:

$$p_{interface,i} = \frac{F_{zeolite,i} p_{feed,i}}{\alpha_i + F_{zeolite,i}} \quad (3)$$

It may also be observed:

$$p_{interface,i} = \frac{J_{molar,i}}{\alpha_i} \quad (4)$$

Inserting

$$p_{interface,i} = \frac{F_{zeolite,i} p_{feed,i}}{\alpha_i + F_{zeolite,i}} \quad (3)$$

into equation (1) :

$$J_{molar,i} = F_{zeolite,i} p_{feed,i} - F_{zeolite,i}\left(\frac{F_{zeolite,i} p_{feed,i}}{\alpha_i + F_{zeolite,i}}\right) \quad (4)$$

Under the conditions of this model:

$$\frac{J_{molar,i}}{p_{feed,i}} = F_{total,i} \quad (5)$$

Rearranging equation (4) results in:

$$\frac{J_{molar,i}}{p_{feed,i}} = F_{zeolite,i}\left(1 - \frac{F_{zeolite,i}}{\alpha_i + F_{zeolite,i}}\right) \quad (6)$$

And:

$$F_{zeolite,i}\left(1 - \frac{F_{z,i}}{\alpha_i + F_{z,i}}\right) = F_{zeolite,i}\left(\frac{\alpha_i}{\alpha_i + F_{zeolite,i}}\right) \quad (7)$$

Therefore:

$$F_{totali} = F_{zeolite,i}\left(\frac{\alpha_i}{\alpha_i + F_{zeolite,i}}\right) \quad (8)$$

Equation (8) can be rearranged:

$$\frac{1}{F_{total,i}} = \frac{1}{\alpha_i} + \frac{1}{F_{zeolite,i}}, \qquad (\beta = 0, p_{p,i} = 0) \quad (9)$$

$$Equation\ (9)\ represents\ the\ resistance\ in\ series\ model$$

And, from (8),

$$F_{total,j} = F_{zeolite,j}\left(\frac{\alpha_j}{\alpha_j + F_{zeolite,j}}\right) \quad (10)$$

Defining model selectivity as

$$S_{i,j,model} = \frac{F_{total,i}}{F_{total,j}} \quad (11)$$

Substituting equations (8) and (10) into equation (11) gives:

$$S_{i,j,model} = \frac{F_{zeolite,i}}{F_{zeolite,j}}\frac{\alpha_i}{\alpha_j}\left(\frac{\alpha_j + F_{zeolite,j}}{\alpha_i + F_{zeolite,i}}\right) \quad (12)$$

Further defining:

$$\frac{F_{zeolite,i}}{F_{zeolite,j}} = S_z \qquad selectivity\ of\ zeolite\ membrane \quad (13)$$

And

$$S_s = \frac{\alpha_i}{\alpha_j} \quad selectivity\ of\ support \quad (14)$$

$$\frac{\alpha_i}{\alpha_j} = \sqrt{\frac{Mw_j}{Mw_i}} \quad (15)$$

And

$$\phi_i = \frac{F_{zeolite,i}}{\alpha_i} \quad (16)$$

And

$$Lin\ number = Ln = \frac{S_s}{S_z} \quad (17)$$

By definition of system parameters, $S_s < S_z$ (18), $Ln < 1$ (19).

Then

$$\frac{F_{zeolite,i}}{F_{zeolite,j}}\frac{\alpha_i}{\alpha_j}\left(\frac{\alpha_j + F_{zeolite,j}}{\alpha_i + F_{zeolite,i}}\right) = S_z S_s \left(\frac{\alpha_j + F_{zeolite,j}}{\alpha_i + F_{zeolite,i}}\right) \quad (20)$$

$$S_z S_s \left(\frac{\alpha_j + F_{zeolite,j}}{\alpha_i + F_{zeolite,i}}\right) = S_z S_s \left(\frac{\alpha_j}{\alpha_i + F_{zeolite,i}} + \frac{F_{z,j}}{\alpha_i + F_{zeolite,i}}\right) \quad (21)$$

$$S_z S_s \left(\frac{\alpha_j}{\alpha_i + F_{zeolite,i}} + \frac{F_{zeolite,j}}{\alpha_i + F_{zeolite,i}}\right) = S_z S_s \left(\frac{\frac{\alpha_j}{\alpha_i}}{1 + \frac{F_{zeolite,i}}{\alpha_i}} + \frac{\frac{F_{zeolite,j}}{F_{zeolite,i}}}{\frac{\alpha_i}{F_{zeolite,i}} + 1}\right) \quad (22)$$

$$S_z S_s \left(\frac{\frac{\alpha_j}{\alpha_i}}{1 + \frac{F_{zeolite,i}}{\alpha_i}} + \frac{\frac{F_{zeolite,j}}{F_{z,i}}}{\frac{\alpha_i}{F_{zeolite,i}} + 1}\right) = S_z S_s \left(\frac{\frac{1}{S_s}}{1 + \phi_i} + \frac{\frac{1}{S_z}}{\frac{1}{\phi_i} + 1}\right) \quad (23)$$

$$S_z S_s \left(\frac{\frac{1}{S_s}}{1+\phi_i} + \frac{\frac{1}{S_z}}{\frac{1}{\phi_i}+1} \right) = \left(\frac{S_z}{1+\phi_i} + \frac{S_s \phi_i}{1+\phi_i} \right) \quad (24)$$

$$\left(\frac{S_z}{1+\phi_i} + \frac{S_s \phi_i}{1+\phi_i} \right) = S_{i,j} \quad (25)$$

$$\frac{S_{i,j,model}}{S_z} = \left(\frac{1}{1+\phi_i} + \frac{S_s \phi_i}{S_z(1+\phi_i)} \right) \quad (26)$$

$$\left(\frac{1}{1+\phi_i} + \frac{S_s \phi_i}{S_z(1+\phi_i)} \right) = \left(\frac{1}{1+\phi_i} + \frac{Ln\phi_i}{(1+\phi_i)} \right) \quad (27)$$

$$\left(\frac{1}{1+\phi_i} + \frac{Ln\phi_i}{(1+\phi_i)} \right) = \frac{1+Ln\phi_i}{1+\phi_i} \quad (28)$$

$$\frac{S_{i,j,model}}{S_z} = \frac{1+Ln\phi_i}{1+\phi_i} \quad (29)$$

The following proof clarifies the relationship between $S_{i,j}$as defined here and $S_{i,j}$ as defined by Baker et al.:

Baker at al. define selectivity when $p_p = 0$:

$$S_{i,j} = \frac{F_{total,i}}{F_{total,j}} \quad (30)$$

$$\frac{F_{total,i}}{F_{total,j}} = \frac{J_{molar,i}(x_j \gamma_j p_j^{sat})}{J_{molar,j}(x_i \gamma_i p_i^{sat})} \quad (31)$$

Therefore:

$$S_{i,j}\ (Baker\ et\ al.) = S_{i,j,model}\ (p_{feed,i} = .(x_i \gamma_i p_i^{sat})) \quad (32)$$

The following proof clarifies this relationship:

$$S_{i,j,model} = S_z \frac{1 + Ln\phi_i}{1 + \phi_i} \quad (33)$$

$$S_z \frac{1 + Ln\phi_i}{1 + \phi_i} = \frac{S_z + S_s\phi_i}{1 + \phi_i} \quad (34)$$

$$S_z = \frac{F_{zeolite,i}}{F_{zeolite,j}} \quad (35)$$

$$\frac{F_{zeolite,i}}{F_{zeolite,j}} = \frac{J_{molar,i}\left(x_j\gamma_j p_j^{sat} - p_{interface,j}\right)}{J_{molar,j}(x_i\gamma_i p_i^{sat} - p_{interface,i})} \quad (36)$$

$$\phi_i = \frac{F_{zeolite,i}}{\alpha_i} \quad (37)$$

$$F_{zeolite,i} = \frac{J_{molar,i}}{(x_i\gamma_i p_i^{sat} - p_{interface,i})} \quad (38)$$

$$\alpha_i = \frac{J_{molar,i}}{p_{interface,i}} \qquad p_{permeate,i} = 0 \quad (39)$$

When the molar flux terms in equations (38) and (39) are identical:

$$\frac{F_{zeolite,i}}{\alpha_i} = \frac{p_{interface,i}}{(x_i\gamma_i p_i^{sat} - p_{interface,i})} \quad (40)$$

$$S_s = \sqrt{\frac{Mw_j}{Mw_i}} \quad (41)$$

$$1 + \phi_i = \frac{x_i\gamma_i p_i^{sat}}{(x_i\gamma_i p_i^{sat} - p_{interface,i})} \quad (42)$$

$$\frac{S_z + S_s\phi_i}{1 + \phi_i} = \frac{\frac{J_{molar,i}\left(x_j\gamma_j p_j^{sat} - p_{interface,j}\right)}{J_{molar,j}(x_i\gamma_i p_i^{sat} - p_{interface,i})} + \sqrt{\frac{Mw_j}{Mw_i}}\left(\frac{p_{interface,i}}{\left(x_i\gamma_i p_i^{sat} - p_{interface,i}\right)}\right)}{\frac{x_i\gamma_i p_i^{sat}}{(x_i\gamma_i p_i^{sat} - p_{interface,i})}} \quad (43)$$

$$\frac{S_z + S_s\phi_i}{1+\phi_i} = \frac{J_{molar,i}\left(x_j\gamma_j p_j^{sat} - p_{interface,j}\right)}{J_{molar,j}x_i\gamma_i p_i^{sat}} + \frac{\sqrt{\frac{Mw_j}{Mw_i}}p_{interface,i}}{x_i\gamma_i p_i^{sat}} \quad (44)$$

$$\frac{J_{molar,i}\left(x_j\gamma_j p_j^{sat} - p_{interface,j}\right)}{J_{molar,j}x_i\gamma_i p_i^{sat}} + \frac{\sqrt{\frac{Mw_j}{Mw_i}}p_{interface,i}}{x_i\gamma_i p_i^{sat}}$$

$$= \frac{J_{molar,i}\left(x_j\gamma_j p_j^{sat} - p_{interface,j}\right) + J_{molar,j}\sqrt{\frac{Mw_j}{Mw_i}}p_{interface,i}}{J_{molar,j}x_i\gamma_i p_i^{sat}} \quad (45)$$

Looking at the numerator of the RHS of equation (45):

$$J_{molar,i}\left(x_j\gamma_j p_j^{sat} - p_{interface,j}\right) + J_{molar,j}\sqrt{\frac{Mw_j}{Mw_i}}p_{interface,i}$$

$$= J_{molar,i}x_j\gamma_j p_j^{sat} - J_{molar,i}p_{interface,j} + J_{molar,j}\sqrt{\frac{Mw_j}{Mw_i}}p_{interface,i} \quad (46)$$

It can be observed:

$$J_{molar,i}p_{interface,j} = J_{molar,j}\sqrt{\frac{Mw_j}{Mw_i}}p_{interface,i} \quad (47)$$

Equation (47) results from:

$$\frac{\alpha_i}{\alpha_j} = \sqrt{\frac{Mw_j}{Mw_i}} \quad (48)$$

And

$$\frac{\alpha_i}{\alpha_j} = \frac{J_{molar,i}p_{interface,j}}{J_{molar,j}p_{interface,i}} \quad (49)$$

Therefore:

$$J_{molar,i}x_j\gamma_j p_j^{sat} - J_{molar,i}p_{interface,j} + J_{j,molar}\sqrt{\frac{Mw_j}{Mw_i}}p_{interface,i} = J_{molar,i}x_j\gamma_j p_j^{sat} \quad (50)$$

And

$$S_{i,j,model} = \frac{J_{molar,i}(x_i\gamma_i p_i^{sat})}{J_{molar,j}x_j\gamma_j p_j^{sat})} \quad (51)$$

$$S_{i,j,model} = S_{i,j}\ as\ defined\ by\ Baker\ et\ al. \quad (52)$$

Temperature dependence of selectivity

In general:

$$F = \frac{\varepsilon}{\tau}\frac{1}{L}\frac{D}{RT} \quad (53)$$

For zeolite:

$$D = K_{z1}\sqrt{\frac{8RT}{\pi Mw}}\exp\left(\frac{-E_d}{RT}\right) \quad (54)$$

Therefore

$$F_{zeolite} = K_{z2}\sqrt{\frac{1}{RTMw}}\exp\left(\frac{-E_d}{RT}\right) \quad (55)$$

Then

$$F_{zeolite,i,T_2}\sqrt{\frac{T_1}{T_2}}\exp\left(\frac{E_{d,i}}{R}\left(\frac{1}{T_1}-\frac{1}{T_2}\right)\right)F_{zeolite,i,T_1} \quad (56)$$

$$S_s = \frac{\alpha_i}{\alpha_j} \quad (57)$$

$$\alpha_{i,T_2} = \sqrt{\frac{T_1}{T_2}}\alpha_{i,T_1} \quad (58)$$

Therefore

$$S_{sT_2} = S_{sT_1} \quad (59)$$

Also:

$$S_{z,T_1} = \frac{F_{zeolite,i,T_1}}{F_{zeolite,j,T_1}} \quad (60)$$

$$S_{z,T_2} = \exp\left(\left(\frac{E_{d,i} - E_{d,j}}{R}\right)\left(\frac{1}{T_1} - \frac{1}{T_2}\right)\right) S_{z,T_1} \quad (61)$$

$$Ln_{T_1} = \frac{S_{sT_1}}{S_{z,T_1}} \quad (62)$$

$$\frac{S_{sT_1}}{S_{z,T_1}} = \frac{S_{sT_2}}{S_{z,T_1}} \quad (63)$$

$$Ln_{T_2} = \frac{S_{sT_2}}{S_{z,T_2}} \quad (64)$$

$$\frac{S_{sT_2}}{S_{z,T_2}} = \frac{1}{\exp\left(\left(\frac{E_{d,i} - E_{d,j}}{R}\right)\left(\frac{1}{T_1} - \frac{1}{T_2}\right)\right)} Ln_{T_1} \quad (65)$$

$$Ln_{T_2} = \frac{1}{\exp\left(\left(\frac{E_{d,i} - E_{d,j}}{R}\right)\left(\frac{1}{T_1} - \frac{1}{T_2}\right)\right)} Ln_{T_1} \quad (66)$$

And

$$\phi_{i,T_1} = \frac{F_{zeolite,i,T_1}}{\alpha_{i,T_1}} \quad (67)$$

$$\phi_{i,T_2} = \exp\left(\frac{E_{d,i}}{R}\left(\frac{1}{T_1} - \frac{1}{T_2}\right)\right) \phi_{i,T_1} \quad (68)$$

Therefore

$$Ln_{T_2}\phi_{i,T_2} = \exp\left(\left(\frac{E_{d,j}}{R}\right)\left(\frac{1}{T_1} - \frac{1}{T_2}\right)\right) Ln_{T_1}\phi_{i,T_1} \quad (69)$$

And:

$$\frac{S_{i,j,T_2}}{S_{z,T_2}} = \frac{1 + \exp(\left(\frac{E_{d,j}}{R}\right)\left(\frac{1}{T_1} - \frac{1}{T_2}\right))Ln_{T_1}\phi_{i,T_1}}{1 + \exp\left(\frac{E_{d,i}}{R}\left(\frac{1}{T_1} - \frac{1}{T_2}\right)\right)\phi_{i,T_1}} \quad (70)$$